

On the Quadratic Phase Quaternion Domain Fourier Transform and on the Clifford algebra of $R^{3,1}$

Sadataka Furui

Faculty of Science and Engineering, Teikyo University

2-17-12 Toyosatodai, Utsunomiya, 320-0003 Japan *

January 17, 2024

Abstract

We study application of the Clifford algebra and the Grassmann algebra to image recognitions in $(3 + 1)D$ using quaternions. We construct a quaternion based wave function model with fermions and bosons of equal degrees of freedom, similar to Cartan's supersymmetric model. The Clifford algebra $\mathcal{A}_{3,1}$ is compared with $\mathcal{A}_{2,1}$ and the model applied to the $(2 + 1)D$ non-destructive testing is extended.

The fixed point lattice actions are calculated for 7 paths in $(3 + 1)D$ space with lengths less than or equal to 8 lattice units.

Comparison with the quaternion time approach of Ariel, quaternion Fourier transform of Hitzer and the tensor renormalization group approach to classical lattice models are also discussed.

1 Introduction

Recently Hitzer[1] argued that a generalizing Castro-Minh-Tuan's "New Convolutions for Quadratic-Phase Fourier Integral Operators and their application"[2] in which Fourier transform is performed in \mathbf{R} space can be extended to quaternion Fourier transform. The quaternion Fourier transform

*E-mail address: furui@umb.teikyo-u.ac.jp

was proposed by Hitzer and Sangwine [3] and explained in the textbook [4]. In [2], a quadratic function

$$Q_{(a,b,c,d,e)}(x, y) := ax^2 + bxy + cy^2 + dx + ey \quad a, b, c, d, e \in \mathbf{R} \quad (1)$$

and the integral

$$(Qf)(x) := \frac{1}{\sqrt{2\pi}} \int_{\mathbf{R}} e^{\sqrt{-1}Q_{(a,b,c,0,0)}(x,y)} f(y) dy \quad (2)$$

was considered. Hitzer proposed that the formula can be generalized to

$$Q_{(a,b,c,d,e)}(x, \omega) = ax^2 + bx \cdot \omega + c|\omega|^2 + d \cdot x + e \cdot \omega, \quad a, b, c \in \mathbf{R}, \quad d, e \in \mathbf{H}, \quad (3)$$

where \mathbf{H} is quaternion, and the integral

$$(Qh)(x) = \frac{1}{(2\pi)^2} \int_{\mathbf{H}} h(x) e^{-IQ(x,\omega)} d^4\omega. \quad (4)$$

In this extension of the Fourier transform of complex number space to quaternion number space have problems, when one considers transformations of the 3D spacial space and 1D time space. Since for (3+1) dimensional vector space E and quadratic form q , Clifford Algebra $\mathcal{A}_{3,1}(E, q)$ is isomorphic to $M_2(\mathbf{H})$ or biquaternion [24].

Ariel[8] discussed quaternion space-time in which four dimensional quaternion time

$$\tau^4 = (i_0, \mathbf{i}_1 \frac{x_1}{c}, \mathbf{i}_2 \frac{x_2}{c}, \mathbf{i}_3 \frac{x_3}{c}) \quad (5)$$

was introduced, where $i_0, \mathbf{i}_1, \mathbf{i}_2, \mathbf{i}_3$ are the basis of a quaternion. The quaternion time interval is defined as

$$\mathbf{t} = t(\cos \theta, \sin \theta) = t(\sqrt{1 - \frac{v^2}{c^2}}, \frac{v}{c}) \quad (6)$$

The Lorentz time dilation was expressed by

$$t = |\mathbf{t}| = \frac{t_0}{\sqrt{1 - \frac{v^2}{c^2}}}, \quad (7)$$

where v is \mathbf{x}/t , the ratio of the space interval and the time interval. In [9], the normed division algebra $(\mathbf{R}, \mathbf{C}, \mathbf{H}, \mathbf{O})$ are postulated to be necessary tools for describing nature, and excluded biquaternions as the tools. In electrodynamics the Liénard-Wiechert potential contains the time delay effect $r \rightarrow r - \mathbf{r} \cdot \mathbf{u}/c$ where \mathbf{u} is the velocity of an observer relative to the frame in which the charge is at rest. It is not clear whether the time delay can be expressed by a single quaternion.

Adler[5, 6] showed conditions for constructing quaternion field theory. I will review Adler's work, and try to extend the theory of propagation of solitonic phonon in (2+1)D Weyl fermion sea[16, 27] to quantum field theory in (4+2)D fermion sea.

The structure of this presentation is as follows. In sec.2, I discuss about Adler's quaternion Fourier transform. In sec.3, Clifford algebra $\mathcal{A}_{2,1}$ and its application and in sec.4 Clifford Algebra of $\mathcal{A}_{3,1}$ is explained.

In sec.5 the structure of paths of (3+1)D fixed point actions used in Quantum Chromodynamics is explained. We use bosonic wave propagation in fermion sea expressed by two quaternions, and extend the method of obtaining actions adopted in (2+1)D, in which $e_1 \wedge e_2$ was interpreted as time direction. We compare the case of time shifts along $e_1 e_4, e_2 e_4$ and that along $e_3 e_4$ which are the bases of $\mathcal{A}_{3,1}$.

In sec.6, a comparison with works of Hitzer, Ariel and others and a perspective of quaternion field theory is discussed.

2 Adler's arguments on Quaternion Fourier Transformation and Hitzer's arguments

Hitzer claimed that using a unit pure quaternion I , ($I^2 = -1$). He assumed that the unit quaternion I commutes with quaternions and derived the delta function rule

$$\begin{aligned} & \frac{1}{(2\pi)^4} \int_H e^{-Ibx \cdot \omega} e^{Iby \cdot \omega} d^4 \omega \\ &= \delta(b(x_r - y_r)) \delta(b(x_i - y_i)) \delta(b(x_j - y_j)) \delta(b(x_k - y_k)), \end{aligned} \quad (8)$$

where $x = x_r + x_i \mathbf{i} + x_j \mathbf{j} + x_k \mathbf{k}$ and $y = y_r + y_i \mathbf{i} + y_j \mathbf{j} + y_k \mathbf{k}$. Products of exponential of pure quaternions is however, a complicated object. For $\lambda = p_0 \phi_0 + p_1 \phi_1 + p_2 \phi_2 + p_3 \phi_3$ and $\lambda' = p_0 \phi'_0 + p_1 \phi'_1 + p_2 \phi'_2 + p_3 \phi'_3$,

$$\frac{1}{(2\pi)^2} \int dpe^{\sqrt{-1}(\lambda - \lambda')} = \delta(\phi - \phi') = \delta(\phi_0 - \phi'_0) \delta(\phi_1 - \phi'_1) \delta(\phi_2 - \phi'_2) \delta(\phi_3 - \phi'_3)$$

Since $(\cos(\lambda + \lambda') + \cos(\lambda - \lambda'))/2 = \cos \lambda \cos \lambda'$ and $(-\cos(\lambda + \lambda') - \cos(\lambda - \lambda'))/2 = \sin \lambda \sin \lambda'$, the real part of $dpe^{\sqrt{-1}(\lambda - \lambda')}$ becomes $dp(\cos \lambda \cos \lambda' + \sin \lambda \sin \lambda')$.

Adler[6] defined for bosonic fields ϕ ,

$$\Psi_{pe}(\phi) = \frac{1}{2\pi} \cos \lambda q_e(p) \quad \Psi_{po}(\phi) = \frac{1}{2\pi} \sin \lambda q_o(p),$$

the completeness relation gives

$$\int dp [\Psi_{pe}(\phi') \bar{\Psi}_{pe}(\phi) + \Psi_{po}(\phi') \bar{\Psi}_{po}(\phi)] = \delta(\phi - \phi')$$

where a unit quaternion q_e or q_o depends on arbitrary ways on p .

The kinetic energy

$$\begin{aligned} H_{kin} = & -\frac{1}{6} \sum_{i=1}^M [2e_1 \left(\frac{\partial}{\partial \phi_1^i} \frac{\partial}{\partial \phi_3^i} - \frac{\partial}{\partial \phi_0^i} \frac{\partial}{\partial \phi_2^i} \right) + 2e_2 \left(\frac{\partial}{\partial \phi_0^i} \frac{\partial}{\partial \phi_1^i} + \frac{\partial}{\partial \phi_2^i} \frac{\partial}{\partial \phi_3^i} \right) \\ & + e_3 \left(\frac{\partial}{\partial \phi_0^i} \frac{\partial}{\partial \phi_0^i} + \frac{\partial}{\partial \phi_3^i} \frac{\partial}{\partial \phi_3^i} - \frac{\partial}{\partial \phi_1^i} \frac{\partial}{\partial \phi_1^i} - \frac{\partial}{\partial \phi_2^i} \frac{\partial}{\partial \phi_2^i} \right)] \\ H_{kin} \Psi_{pe} = & \Psi_{pe} \lambda_e(p), \quad H_{kin} \Psi_{po} = \Psi_{po} \lambda_o(p) \end{aligned} \quad (9)$$

$\lambda_{e,o}(p)$ can be expressed as

$$\lambda_{e,o}(p) = \frac{1}{6} (p_0^2 + p_1^2 + p_3^2) e_{e,o}(p)$$

where $e_{e,o}$ is the unit pure(imaginary) quaternion, which can be given any orientation by an appropriate choice of $q_{e,o}(p)$.

Since the generalized Quadratic Phase Quaternion Domain Fourier Transform (QPQDFT) must contain Adler's specific case, it is likely that the 2D split structure remains and the integral over d^2p instead of d^4p plays essential roles.

Cartan[7] showed in the ν dimensional Euclidean space E_ν , there exists vectors x_1, \dots, x_ν , x'_1, \dots, x'_ν and semi-spinors $\xi_0, \xi_{23}, \xi_{31}, \xi_{12}$ and $\xi_{123}, -\xi_1, -\xi_2, -\xi_3$ and they are supersymmetric relations.

When $\nu = 3$,

$$x_1 = \xi_{31} \xi'_{12} - \xi_{12} \xi_{31}, \quad x_2 = \xi_{12} \xi_{23} - \xi_{23} \xi'_{12}, \quad x_3 = \xi_{23} \xi'_{31} - \xi_{31} \xi'_{23} \quad (10)$$

$$x'_1 = \xi_0 \xi'_{23} - \xi_{23} \xi'_0, \quad x'_2 = \xi_0 \xi'_{31} - \xi_{31} \xi'_0, \quad x'_3 = \xi_0 \xi'_{12} - \xi_{12} \xi'_0. \quad (11)$$

and

$$x_1 = \xi_{123} \xi'_1 - \xi_1 \xi_{123}, \quad x_2 = \xi_{123} \xi'_2 - \xi_2 \xi'_{123}, \quad x_3 = \xi_{123} \xi'_3 - \xi_3 \xi'_{123} \quad (12)$$

$$x'_1 = \xi_3 \xi'_2 - \xi_2 \xi'_3, \quad x'_2 = \xi_1 \xi'_3 - \xi_3 \xi'_1, \quad x'_3 = \xi_2 \xi'_1 - \xi_1 \xi'_2 \quad (13)$$

When $\nu = 4$, there are invariant coupling of vectors and semi-spinors

$$\begin{aligned}
\varphi^T C X \psi = & x^1(\xi_{12}\xi_{314} - \xi_{31}\xi_{134} - \xi_{14}\xi_{123} + \xi_{1234}\xi_1) \\
& + x^2(\xi_{23}\xi_{124} - \xi_{12}\xi_{234} - \xi_{34}\xi_{123} + \xi_{1234}\xi_2) \\
& + x^3(\xi_{31}\xi_{234} - \xi_{23}\xi_{314} - \xi_{34}\xi_{123} + \xi_{1234}\xi_3) \\
& + x^4(-\xi_{14}\xi_{234} - \xi_{24}\xi_{314} - \xi_{34}\xi_{124} + \xi_{1234}\xi_4) \\
& + x'_1(-\xi_0\xi_{234} + \xi_{23}\xi_4 - \xi_{34}\xi_3 + \xi_{34}\xi_2) \\
& + x'_2(-\xi_0\xi_{314} + \xi_{31}\xi_4 - \xi_{34}\xi_1 + \xi_{14}\xi_3) \\
& + x'_3(-\xi_0\xi_{124} + \xi_{12}\xi_4 - \xi_{14}\xi_2 + \xi_{24}\xi_1) \\
& + x'_4(\xi_0\xi_{123} - \xi_{23}\xi_1 - \xi_{31}\xi_2 - \xi_{12}\xi_3)
\end{aligned} \tag{14}$$

In the case of $\nu = 4$, $x_4 \rightarrow -x'_4$ transformation exists in the G_{23} group. The G_{12} and G_{13} groups supersymmetric transformations between x and ξ exist.

In performing quaternion Fourier transform, we choose discrete lattices with a certain time and a coordinate system expressed by pure quaternions. A pure quaternion $q = xe_1 + ye_2 + ze_3$, $(x, y, z) \in R$ is chosen as $x^2 + y^2 + z^2 = 1$ and its conjugate is $\bar{q} = -xe_1 - ye_2 - ze_3$. The orthogonal 2D planes split (OPS) [3] consists of deviding

$$q = q_+ + q_-, \quad q_{\pm} = \frac{1}{2}(q \pm e_1 q e_2). \tag{15}$$

The Hilbert space is constructed as patching the quaternion on S^4 around the discretized time series, and as Kodaira[10] construct the K  hler structure on the complex projected space.

3 Clifford Algebra of (2+1)D

In the (2+1)D Clifford action lattice simulation, the link operator of direction e_1 , length a , from the position (u_1, u_2) is calculated in Mathematica, by using $X = \begin{pmatrix} x & xx^- \\ I_2 & x^- \end{pmatrix}$, where I_2 is the 2×2 diagonal unit matrix. The hyperplane reflection $x \rightarrow -x^-$ is represented by a multiplication of $\begin{pmatrix} 0 & 1 \\ -1 & 0 \end{pmatrix}$, a shift of length c is realized by using an operator $\mathcal{T} = \begin{pmatrix} I_2 & c \\ 0 & I_2 \end{pmatrix}$ as $\mathcal{T}.X.\mathcal{T}^{-1}$

The coordinate X is represented by (u_1, u_2) as

$$X(u_1, u_2) = \begin{pmatrix} \sqrt{-1}u_1 & u_2 & \sqrt{-1}u_1^2 - u_1u_2 & u_1u_2 + \sqrt{-1}u_2^2 \\ -u_2 & -\sqrt{-1}u_1 & -u_1u_2 - \sqrt{-1}u_2^2 & -\sqrt{-1}u_1^2 + u_1u_2 \\ 1 & 0 & u_1 + \sqrt{-1}u_2 & 0 \\ 0 & 1 & 0 & u_1 + \sqrt{-1}u_2 \end{pmatrix} \quad (16)$$

For getting the information of anomalous scattering positions, we adopted fast Fourier Transform(FFT) of actions along the u_i axes ($i = 1, 2$) obtained from each loops[16].

In signal processing[12], there is a Fourier transform method using the Riesz wavelet transform[14]. The wavelet transform is different from FFT in taking into account the shape of amplitudes squared. The Riesz transform in 2D is expressed as first calculate

$$\mathbf{f}_R(\mathbf{x}) = \begin{pmatrix} f_1(\mathbf{x}) \\ f_2(\mathbf{x}) \end{pmatrix} = \begin{pmatrix} h_x * f(\mathbf{x}) \\ h_y * f(\mathbf{x}) \end{pmatrix} \quad (17)$$

where $\mathbf{x} = (x, y)$ is the input signal, $h_x(\mathbf{x}) = x/(2\pi||\mathbf{x}||^3)$, $h_y(\mathbf{x}) = y/(2\pi||\mathbf{x}||^3)$ [14].

In the TR-NEWS, convolution of signals with windows functions, which are different from h_x and h_y are used, and we adopt the short-time Fourier transform (STFT)[15].

$$\text{STFT}\{x(t)\}(\tau, \omega) \equiv X(\tau, \omega) = \int_{-\infty}^{\infty} x(t)w(t - \tau)e^{-\sqrt{-1}\omega t}dt \quad (18)$$

The discrete time STFT is

$$\text{STFT}\{x[n]\}(m, \omega) = \sum_{n=-\infty}^{\infty} x[n]w[n - m]e^{-\sqrt{-1}\omega n} \quad (19)$$

Inverse STFT is

$$x(t)w(t - \tau) = \frac{1}{2\pi} \int_{-\infty}^{\infty} X(\tau, \omega)e^{+\sqrt{-1}\omega t}d\omega. \quad (20)$$

An extension to $(3 + 1)D$ will be discussed in sec.6.

4 Clifford Algebra of (3+1)D

A mapping $R^3 \rightarrow R^{3,1}$ is obtained by taking $u_1 = x, u_2 = y, u_3 = z$, and a vector $X \in R^{3,1}$ is expressed as

$$X = xe_1 + ye_2 + ze_3 + te_4, \quad (21)$$

In $R^{3,1}$, the basis are 4×4 matrices[19]

$$\begin{aligned} e_1 &= \begin{pmatrix} 1 & 0 & 0 & 0 \\ 0 & -1 & 0 & 0 \\ 0 & 0 & -1 & 0 \\ 0 & 0 & 0 & 1 \end{pmatrix}, & e_2 &= \begin{pmatrix} 0 & 1 & 0 & 0 \\ 1 & 0 & 0 & 0 \\ 0 & 0 & 0 & 1 \\ 0 & 0 & 1 & 0 \end{pmatrix}, \\ e_3 &= \begin{pmatrix} 0 & 0 & 1 & 0 \\ 0 & 0 & 0 & -1 \\ 1 & 0 & 0 & 0 \\ 0 & -1 & 0 & 0 \end{pmatrix}, & e_4 &= \begin{pmatrix} 0 & -1 & 0 & 0 \\ 1 & 0 & 0 & 0 \\ 0 & 0 & 0 & -1 \\ 0 & 0 & 1 & 0 \end{pmatrix}. \end{aligned} \quad (22)$$

$e_1 = -e_2e_3, e_2 = -e_3e_1, e_3 = -e_1e_2$ are the bases of $Cl_3^+[19]$, or $\mathcal{A}_3^+[24]$. The sum of the products $e_i\bar{e}_i + \bar{e}_ie_i$ is 0 due to anti-commutativity of quaternions.

In analogy to the $(2+1)D$ case, one could map x, y, z, t on S^4 as

$$X = \frac{2u_1}{1+|u|^2}e_1 + \frac{2u_2}{1+|u|^2}e_2 + \frac{2u_3}{1+|u|^2}e_3 + \frac{1-|u|^2}{1+|u|^2}e_4, \quad (23)$$

where $|u|^2 = u_1^2 + u_2^2 + u_3^2$.

Hitzer and Sangwine's[3] OPS of quaternion space suggests that not only e_4, e_3 , but also e_4, e_1 and e_4, e_2 can be chosen as the split bases.

We define a reflection matrix $\text{ref} = \begin{pmatrix} 0 & 0 & 1 & 0 \\ 0 & 0 & 0 & -1 \\ 1 & 0 & 0 & 0 \\ 0 & -1 & 0 & 0 \end{pmatrix}$ and define $\bar{e}_i = -\text{ref}.e_i$

$(i = 1, \dots, 4)$. For $i = 1, 2, 3$ $e_i.\bar{e}_i = \begin{pmatrix} 0 & I_2 \\ -I_2 & 0 \end{pmatrix}$ and $e_4.\bar{e}_4 = \begin{pmatrix} 0 & -I_2 \\ I_2 & 0 \end{pmatrix}$.

The sign difference of $e_4.\bar{e}_4$ matches the Minkowski's metric.

Following the conformal treatment of Clifford algebra[22], we define

$$\mathcal{X} = \begin{pmatrix} X & X\bar{X} \\ I_4 & \bar{X} \end{pmatrix} \quad (24)$$

where I_4 is 4 dimensional diagonal matrix. When there is one quaternion, the method of sandwiching \mathcal{X} between extended Vahlen matrices [21], adopted in $(2+1)D$ works.

Lounesto[19] and Vaz[20] defined a vector in $Cl_3 \simeq M_2(\mathbf{C})$ as

$$u = u_0 + u_1 e_1 + u_2 e_2 + u_3 e_3 + u_{12} e_{12} + u_{13} e_{13} + u_{23} e_{23} + u_{123} e_{123} \quad (25)$$

and for an even element $u \in Cl_3^+$ and 4 dimensional base (f_1, f_2, f_3, f_4) , expressed

$$\begin{aligned} u\psi &= (u_0 + u_1 e_{23} + u_2 e_{31} + u_3 e_{23})(\psi_0 f_0 + \psi_1 f_1 + \psi_2 f_2 + \psi_3 f_3) \\ &\simeq \begin{pmatrix} u_0 & -u_1 & -u_2 & -u_3 \\ u_1 & u_0 & u_3 & -u_2 \\ u_2 & -u_3 & u_0 & u_1 \\ u_3 & u_2 & -u_1 & u_0 \end{pmatrix} \begin{pmatrix} \psi_0 \\ \psi_1 \\ \psi_2 \\ \psi_3 \end{pmatrix} \end{aligned} \quad (26)$$

and showed $Cl_3^+ \simeq \mathbf{H}$. Vaz described the electron's Dirac equation in the form

$$\sqrt{-1}\hbar(\partial_t + \alpha^k \partial_k)\psi = m\beta(\psi), \quad (27)$$

where

$$\beta(\alpha^i \psi) + \alpha^i \beta(\psi) = 0, \quad i = 1, 2, 3 \quad (28)$$

$$(\sqrt{-1}\beta)^2(\psi) = \sqrt{-1}\beta(\sqrt{-1}\beta(\psi)) = -\psi. \quad (29)$$

The author claimed by a proper choice of β , α^k can be chosen as the Pauli matrices.

There are discussions on the β in more general framework by Hestenes[23].

The algebra in $R^{3,1}$ is not isomorphic to one quaternion. The algebra $\mathcal{A}_{3,1}$ is isomorphic to $M_2(\mathbf{H})$.

Garling [24] performed the mapping $\tilde{\gamma} = R^{3,1} \rightarrow M_2(\mathbf{C})$ as Dyson[18]

$$x = \lambda_0 I + \sum_{1 \leq i < j \leq 4} \lambda_{ij} e_i e_j + \lambda_\Omega e_\Omega \quad (30)$$

and set $p = \lambda_0 + \sqrt{-1}\lambda_\Omega$, $q = -(\lambda_{13} + \sqrt{-1}\lambda_{34})$, $r = -(\lambda_{14} + \sqrt{-1}\lambda_{23})$, $s = -(\lambda_{34} + \sqrt{-1}\lambda_{12})$ for the mapping equivalent to $M_2(\mathbf{C})$.

Here

$$e_2 e_3 = \begin{pmatrix} 0 & -\sqrt{-1} & 0 & 0 \\ -\sqrt{-1} & 0 & 0 & 0 \\ 0 & 0 & 0 & \sqrt{-1} \\ 0 & 0 & \sqrt{-1} & 0 \end{pmatrix}, \quad e_1 e_3 = \begin{pmatrix} 0 & 1 & 0 & 0 \\ -1 & 0 & 0 & 0 \\ 0 & 0 & 0 & 1 \\ 0 & 0 & -1 & 0 \end{pmatrix} \quad (31)$$

$$e_1e_2 = \begin{pmatrix} -\sqrt{-1} & 0 & 0 & 0 \\ 0 & \sqrt{-1} & 0 & 0 \\ 0 & 0 & -\sqrt{-1} & 0 \\ 0 & 0 & 0 & \sqrt{-1} \end{pmatrix}, \quad e_1e_4 = \begin{pmatrix} 0 & -1 & 0 & 0 \\ -1 & 0 & 0 & 0 \\ 0 & 0 & 0 & 1 \\ 0 & 0 & 1 & 0 \end{pmatrix} \quad (32)$$

$$e_2e_4 = \begin{pmatrix} 0 & \sqrt{-1} & 0 & 0 \\ -\sqrt{-1} & 0 & 0 & 0 \\ 0 & 0 & 0 & \sqrt{-1} \\ 0 & 0 & -\sqrt{-1} & 0 \end{pmatrix}, \quad e_3e_4 = \begin{pmatrix} -1 & 0 & 0 & 0 \\ 0 & 1 & 0 & 0 \\ 0 & 0 & 1 & 0 \\ 0 & 0 & 0 & -1 \end{pmatrix} \quad (33)$$

For $x = \lambda_0 I + \sum_{1 \leq i < j \leq 4} \lambda_{ij} e_i e_j$, and the Dirac matrices described by

$$Q = \begin{pmatrix} 0 & 1 \\ 1 & 0 \end{pmatrix}, J = \begin{pmatrix} 0 & -1 \\ 1 & 0 \end{pmatrix}, U = \begin{pmatrix} 1 & 0 \\ 0 & -1 \end{pmatrix} \quad (34)$$

as

$$\gamma(e_1e_3) = -J \otimes I = \begin{pmatrix} 0 & 0 & 1 & 0 \\ 0 & 0 & 0 & 1 \\ -1 & 0 & 0 & 0 \\ 0 & -1 & 0 & 0 \end{pmatrix} \quad (35)$$

$$\gamma(e_2e_4) = -\sqrt{-1}J \otimes U = \begin{pmatrix} 0 & 0 & \sqrt{-1} & 0 \\ 0 & 0 & 0 & -\sqrt{-1} \\ -\sqrt{-1} & 0 & 0 & 0 \\ 0 & \sqrt{-1} & 0 & 0 \end{pmatrix} \quad (36)$$

$$\gamma(e_1e_4) = -Q \otimes U = \begin{pmatrix} 0 & 0 & -1 & 0 \\ 0 & 0 & 0 & 1 \\ -1 & 0 & 0 & 0 \\ 0 & 1 & 0 & 0 \end{pmatrix} \quad (37)$$

$$\gamma(e_2e_3) = -\sqrt{-1}Q \otimes I = \begin{pmatrix} 0 & 0 & -\sqrt{-1} & 0 \\ 0 & 0 & 0 & -\sqrt{-1} \\ -\sqrt{-1} & 0 & 0 & 0 \\ 0 & -\sqrt{-1} & 0 & 0 \end{pmatrix} \quad (38)$$

$$\gamma(e_3e_4) = -U \otimes U = \begin{pmatrix} -1 & 0 & 0 & 0 \\ 0 & 1 & 0 & 0 \\ 0 & 0 & 1 & 0 \\ 0 & 0 & 0 & -1 \end{pmatrix} \quad (39)$$

$$\gamma(e_1e_2) = -\sqrt{-1}U \otimes I = \begin{pmatrix} -\sqrt{-1} & 0 & 0 & 0 \\ 0 & -\sqrt{-1} & 0 & 0 \\ 0 & 0 & \sqrt{-1} & 0 \\ 0 & 0 & 0 & \sqrt{-1} \end{pmatrix} \quad (40)$$

$$\gamma(x) - \lambda_0 I_4 = \begin{pmatrix} -t & 0 & u-v & 0 \\ 0 & \bar{t} & 0 & \bar{u}+\bar{v} \\ -u-v & 0 & t & 0 \\ 0 & -\bar{u}+\bar{v} & 0 & -\bar{t} \end{pmatrix} \quad (41)$$

where $t = \lambda_{34} + \sqrt{-1}\lambda_{12}$, $u = \lambda_{13} + \sqrt{-1}\lambda_{24}$, $v = \lambda_{14} + \sqrt{-1}\lambda_{23}$.

The reflections of e_ie_j are denoted as $\overline{e_ie_j}$.

$$\overline{e_2e_3} = \begin{pmatrix} 0 & 0 & 0 & \sqrt{-1} \\ 0 & 0 & -\sqrt{-1} & 0 \\ 0 & -\sqrt{-1} & 0 & 0 \\ \sqrt{-1} & 0 & 0 & 0 \end{pmatrix}, \quad \overline{e_1e_3} = \begin{pmatrix} 0 & 0 & 0 & 1 \\ 0 & 0 & 1 & 0 \\ 0 & 1 & 0 & 0 \\ 1 & 0 & 0 & 0 \end{pmatrix} \quad (42)$$

$$\overline{e_1e_2} = \begin{pmatrix} 0 & 0 & -\sqrt{-1} & 0 \\ 0 & 0 & 0 & -\sqrt{-1} \\ -\sqrt{-1} & 0 & 0 & 0 \\ 0 & -\sqrt{-1} & 0 & 0 \end{pmatrix}, \quad \overline{e_1e_4} = \begin{pmatrix} 0 & 0 & 0 & 1 \\ 0 & 0 & -1 & 0 \\ 0 & -1 & 0 & 0 \\ 1 & 0 & 0 & 0 \end{pmatrix} \quad (43)$$

$$\overline{e_2 e_4} = \begin{pmatrix} 0 & 0 & 0 & \sqrt{-1} \\ 0 & 0 & \sqrt{-1} & 0 \\ 0 & \sqrt{-1} & 0 & 0 \\ \sqrt{-1} & 0 & 0 & 0 \end{pmatrix}, \quad \overline{e_3 e_4} = \begin{pmatrix} 0 & 0 & 1 & 0 \\ 0 & 0 & 0 & 1 \\ -1 & 0 & 0 & 0 \\ 0 & -1 & 0 & 0 \end{pmatrix}. \quad (44)$$

The product of the multiple and its reflection is

$$\begin{aligned} e_1 e_2 \cdot \overline{e_1 e_2} &= -e_1 e_3 \cdot \overline{e_1 e_3} = e_1 e_4 \cdot \overline{e_1 e_4} = -e_2 e_3 \cdot \overline{e_2 e_3} = e_2 e_4 \cdot \overline{e_2 e_4} = -e_3 e_4 \cdot \overline{e_3 e_4} \\ &= \begin{pmatrix} 0 & 0 & -1 & 0 \\ 0 & 0 & 0 & 1 \\ -1 & 0 & 0 & 0 \\ 0 & 1 & 0 & 0 \end{pmatrix} \end{aligned} \quad (45)$$

The shift transformation becomes $\mathcal{T}X\mathcal{T}^{-1} = X'$, where $\mathcal{T} = \begin{pmatrix} I_4 & c \\ 0 & I_4 \end{pmatrix}$, and modify c suggested by Garling[24]

$$c = c_{23}e_2e_3 + c_{13}e_1e_3 + c_{12}e_1e_2 + c_{14}e_1e_4 + c_{24}e_2e_4 + c_{34}e_3e_4 + c_0I + c_\Omega e_\Omega, \quad (46)$$

for calculation of actions in (3+1)D, this 8 dimensional shift vector is not suitable.

Therefore we replace the base e_1 by e_2e_3 , e_2 by e_3e_1 , e_3 by e_1e_2 . The e_4 is replaced by e_1e_4, e_2e_4 or e_3e_4 .

Therefore we choose shift vectors in (3+1)D as

$$\begin{aligned} c_1 &= c_{23}e_2e_3 + c_{13}e_1e_3 + c_{12}e_1e_2 + c_{14}e_1e_4 \\ c_2 &= c_{23}e_2e_3 + c_{13}e_1e_3 + c_{12}e_1e_2 + c_{24}e_2e_4 \\ c_3 &= c_{23}e_2e_3 + c_{13}e_1e_3 + c_{12}e_1e_2 + c_{34}e_3e_4 \end{aligned} \quad (47)$$

and corresponding momentum space position vectors

$$\begin{aligned} x_1 &= xe_2e_3 + ye_1e_3 + ze_1e_2 + te_1e_4 \\ x_2 &= xe_2e_3 + ye_1e_3 + ze_1e_2 + te_2e_4 \\ x_3 &= xe_2e_3 + ye_1e_3 + ze_1e_2 + te_3e_4. \end{aligned} \quad (48)$$

When the time component is te_ie_4 and $t\overline{e_ie_4}$, ($i = 1, 2, 3$), we define

$$\Phi_i = \begin{pmatrix} X_i & X_i \bar{X}_i \\ I_4 & \bar{X}_i \end{pmatrix}, \quad (49)$$

where I_4 is a 4 dimensional diagonal matrix, and X_i, \bar{X}_i are 4×4 matrices.

When the time component is te_1e_4 and $t\overline{e_1e_4}$,

$$X_1 = \begin{pmatrix} -\sqrt{-1}z & -t - \zeta & 0 & 0 \\ -t + \bar{\zeta} & \sqrt{-1}z & 0 & 0 \\ 0 & 0 & -\sqrt{-1}z & t - \bar{\zeta} \\ 0 & 0 & t + \zeta & \sqrt{-1}z \end{pmatrix}, \bar{X}_1 = \begin{pmatrix} 0 & 0 & -\sqrt{-1}z & t - \bar{\zeta} \\ 0 & 0 & -t - \zeta & -\sqrt{-1}z \\ -\sqrt{-1}z & -t - \zeta & 0 & 0 \\ t - \bar{\zeta} & -\sqrt{-1}z & 0 & 0 \end{pmatrix} \quad (50)$$

where $\zeta = \sqrt{-1}x - y, \bar{\zeta} = -\sqrt{-1}x - y$.

$$X_1 \bar{X}_1 = \begin{pmatrix} 0 & 0 & (t + \zeta)^2 - z^2 & -2\sqrt{-1}yz \\ 0 & 0 & 2\sqrt{-1}yz & -(t - \bar{\zeta})^2 + z^2 \\ (t - \bar{\zeta})^2 - z^2 & -2\sqrt{-1}yz & 0 & 0 \\ 2\sqrt{-1}yz & -(t + \zeta)^2 + z^2 & 0 & 0 \end{pmatrix} \quad (51)$$

When the time component is te_2e_4 and $t\overline{e_2e_4}$,

$$X_2 = \begin{pmatrix} -\sqrt{-1}z & \sqrt{-1}t - \zeta & 0 & 0 \\ \sqrt{-1}t + \bar{\zeta} & \sqrt{-1}z & 0 & 0 \\ 0 & 0 & -\sqrt{-1}z & \sqrt{-1}t - \bar{\zeta} \\ 0 & 0 & -\sqrt{-1}t - \bar{\zeta} & \sqrt{-1}z \end{pmatrix} \quad (52)$$

$$\bar{X}_2 = \begin{pmatrix} 0 & 0 & -\sqrt{-1}z & \sqrt{-1}t - \bar{\zeta} \\ 0 & 0 & \sqrt{-1}t - \zeta & -\sqrt{-1}z \\ -\sqrt{-1}z & \sqrt{-1}t - \zeta & 0 & 0 \\ \sqrt{-1}t - \bar{\zeta} & -\sqrt{-1}z & 0 & 0 \end{pmatrix}. \quad (53)$$

$$X_2 \bar{X}_2 = \begin{pmatrix} 0 & 0 & (\sqrt{-1}t - \zeta)^2 - z^2 & 2(t - \sqrt{-1}y)z \\ 0 & 0 & -2(t - \sqrt{-1}y)z & -(\sqrt{-1}t - \bar{\zeta})^2 + z^2 \\ (\sqrt{-1}t - \zeta)^2 - z^2 & 2(t - \sqrt{-1}y)z & 0 & 0 \\ -2(t - \sqrt{-1}y)z & -(\sqrt{-1}t - \zeta)^2 + z^2 & 0 & 0 \end{pmatrix} \quad (54)$$

When the time component is te_3e_4 and $\overline{te_3e_4}$,

$$X_3 = \begin{pmatrix} -t - \sqrt{-1}z & -\zeta & 0 & 0 \\ \bar{\zeta} & t + \sqrt{-1}z & 0 & 0 \\ 0 & 0 & t - \sqrt{-1}z & -\bar{\zeta} \\ 0 & 0 & \zeta & -t + \sqrt{-1}z \end{pmatrix} \quad (55)$$

$$\bar{X}_3 = \begin{pmatrix} 0 & 0 & t - \sqrt{-1}z & -\bar{\zeta} \\ 0 & 0 & -\zeta & t - \sqrt{-1}z \\ -t - \sqrt{-1}z & -\zeta & 0 & 0 \\ -\bar{\zeta} & -t - \sqrt{-1}z & 0 & 0 \end{pmatrix}. \quad (56)$$

$$X_3 \bar{X}_3 = \begin{pmatrix} 0 & 0 & \zeta^2 - t^2 - z^2 & -2\sqrt{-1}(tx + yz) \\ 0 & 0 & -2\sqrt{-1}(tx - yz) & -\zeta^2 + t^2 + z^2 \\ \zeta^2 - t^2 - z^2 & -2\sqrt{-1}(tx + yz) & 0 & 0 \\ -2\sqrt{-1}(tx - yz) & -\zeta^2 + t^2 + z^2 & 0 & 0 \end{pmatrix} \quad (57)$$

Dyson pointed out that for a quaternion [18]

$$q = \begin{pmatrix} a & b \\ c & d \end{pmatrix}, \quad \bar{q} = \begin{pmatrix} d & -b \\ -c & a \end{pmatrix}, \quad \tau_3 = \begin{pmatrix} \sqrt{-1} & 0 \\ 0 & -\sqrt{-1} \end{pmatrix}, \quad (58)$$

$$\bar{q}\tau_3q = \sqrt{-1} \begin{pmatrix} bc + ad & 2bd \\ -2ac & -bc - ad \end{pmatrix} \quad (59)$$

becomes a pure imaginary matrix.

In the present work, we do not consider gauge actions and consider propagation of Bosonic solitons in fermion sea.

In lattice simulations we consider paths that start from a point in space-time and return to the starting point which contain time axes. The continuation of a path of direction $e_i e_j$ and $e_k e_l$ is chosen such that either $i = k$ or l , or either $j = k$ or l and the time axis is chosen one of $e_1 e_4$, $e_2 e_4$ and $e_3 e_4$. The step 8 returns to the step 0 cyclically.

5 Fixed Point actions in (3+1)D

The Fixed Point (FP) actions are characterized by spacial lattice unit $\Delta_u = \frac{1}{2^{n+2}}$ and time step unit δ . The loops starts from $(x, y, z, t) = (i, j, k, 0)$, and returns to the initial position. Loops of DeGrand et al.[34] that contain links of both z and t are $L19, L20, L21, L22, L23, L24, L25$.

The paths $L19 - 25$ considered by DeGrand et al[34] are shown in Fig. 1,2,3,4,5,6 and Fig.7. A pair of balls at edges is the position where time shifts (hysteresis effects) occur.

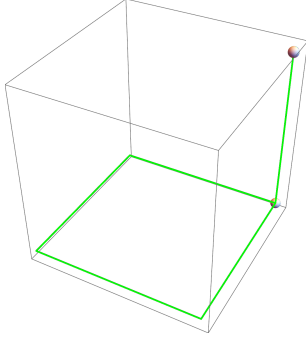


Figure 1: $L19$. The upper right corner ball is $e_2 e_4$, the lower right corner one is $-e_2 e_4$

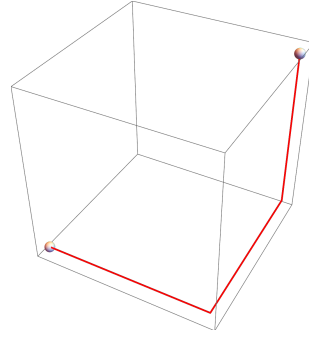


Figure 2: $L20$. The upper right corner ball is $e_2 e_4$, the lower left corner one is $-e_2 e_4$

The 7 FP actions that contain paths along the t axis are shown in the Table 1. there are ambiguity in the choice of $e_1 e_4$ or $e_2 e_4$, but we choose one if there is a partner of the opposite time direction,

Since $e_1 e_4$, $e_2 e_4, e_3 e_4$ have different space-time transformations, when the partner of $e_k e_4$ is $-e_j e_4$ ($j \neq k$), nontrivial transformations appear.

In the case of $L19$, the step 5 is fixed to be $-e_2 e_4$, and the step 3 is fixed to be $e_2 e_4$. Similarly in $L25$, $\pm e_2 e_4$ pair appear.

In the case of $L20$, the step 7 is $-e_2 e_4$ and the step 3 is fixed to be $e_2 e_4$.

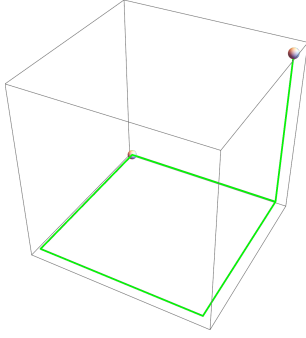


Figure 3: L21. The upper right corner ball is e_1e_4/e_2e_4 , the lower left corner one is $-e_3e_4$.

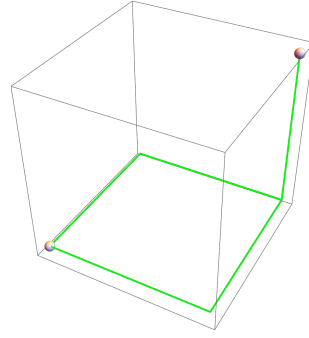


Figure 4: L22. The upper right corner ball is e_1e_4/e_2e_4 , the lower left corner one is $-e_3e_4$.

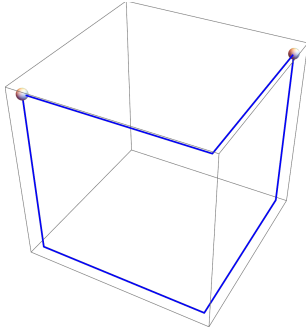


Figure 5: L23. The upper right corner ball is e_1e_4 , the upper left corner one is $-e_2e_4$.

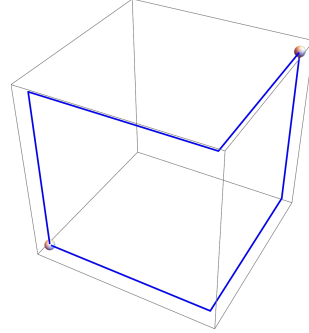


Figure 6: L24. The upper right corner ball is e_1e_4 , the lower left corner one is $-e_2e_4$.

In the case of $L21$ and $L22$, both e_1e_2 or e_2e_1 partner is $-e_3e_4$.

In the case of $L23$ and $L24$, e_1e_4 , $-e_2e_4$ pair appear.

In the table 1, among $7 \pm e_i e_4$ pairs there are 2 $-e_3e_4$ and 12 e_1e_4 or e_2e_4 pairs.

step	0	1	2	3	4	5	6	7
L19	x	y	z	t	-z	-t	-x	-y
	23	31	12	24	-12	-24	-23	-31
L20	x	y	z	t	-z	-y	-x	-t
	23	31	12	24	-12	-31	-23	-24
L25	x	y	z	t	-x	-y	-z	-t
	23	31	12	24	-23	-13	-12	-24

Table 1. Directions of the wave front of loops L19, L20, L25

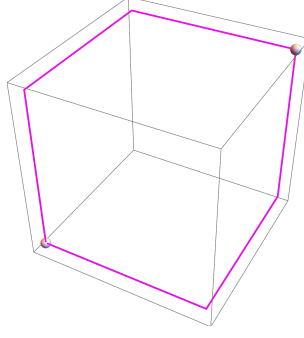


Figure 7: L25. The upper right corner ball is e_2e_4 , the lower left corner one is $-e_2e_4$

• L21

x	y	z	t	-z	-x	-t	-y	-x	-y	-z	-t	z	x	t	y
23	31	12	14/24	-12	-23	-34	-13	-23	-31	-12	-14/24	12	23	34	13

• L22

x	y	z	t	-z	-x	-y	-t	-x	-y	-z	-t	z	x	y	t
23	31	12	14/24	-12	-23	-31	-34	-23	-31	-12	-14/24	12	23	31	34

• L23

x	y	z	t	-y	-x	-t	-z	-x	-y	-z	-t	y	x	t	z
23	31	12	14	-31	-23	-24	-12	-23	-31	-12	-14	31	23	24	12

• L24

x	y	z	t	-y	-x	-z	-t	-x	-y	-z	-t	y	x	z	t
23	31	12	14	-31	-23	-12	-24	-23	-31	-12	-14	31	23	12	24

Table 2. Directions of the wave front of loops in the e_1, e_2, e_3, e_4 bases (the first line) and in the e_ie_j bases (the second line) of $L21, L22, L23$ and $L24$.

The first line of each loop indicates the direction of the wave front. The second line indicates ij of the basis e_ie_j of the $R^{3,1} \simeq M_2(\mathbf{H})$. The transformations are chosen such that i or j of subsequent e_ie_j is equal, and that e_ie_4 and $-e_ie_4$ appear in the sequences.

The path of $L19, L20, L21, L22$ are shown in Fig.1, 2, 3, 4 respectively.

The path of $L23, L24, L25$ are shown in Fig.5, 6, 7 respectively.

In the calculation of 7 loop actions, we choose 3 random numbers (u_1, u_2, u_3) each in $(0, 1)$ and calculate (s_1, s_2, s_3, s_4) in $(0, \Delta_u)$. Then we choose 8 random numbers $(a_1, a_2, b_1, b_2, c_1, c_2, d_1, d_2)$

each in $(0, 1)$ of arbitrary number of sets. As a test I chose 4 sets.

- 1) Define $\tilde{j}_1 = j + s_1, x_1 = \tilde{j}_1 e_2 e_3, \bar{x}_1 = \tilde{j}_1 \overline{e_2 e_3}$ and $X_1 = \begin{pmatrix} x_1 & x_1 \bar{x}_1 \\ I_4 & \bar{x}_1 \end{pmatrix}$.

$$\text{Define } V_1 = \begin{pmatrix} a_1 I_4 & b_1 e_2 e_3 \\ c_1 e_2 e_3 & 0 \end{pmatrix} \text{ and } V_1^\dagger = \begin{pmatrix} 0 & c_1 \overline{e_2 e_3} \\ b_1 \overline{e_2 e_3} & a_1 \bar{I}_4 \end{pmatrix}$$

Calculate $V_1 X_1 V_1^\dagger - X_1$.

- 2) Define $\tilde{j}_2 = j_0 + s_2, x_2 = \tilde{j}_1 e_2 e_3 + \tilde{j}_2 e_1 e_3, \bar{x}_2 = \tilde{j}_1 \overline{e_2 e_3} + \tilde{j}_2 \overline{e_1 e_3}$, where j_0 is a fixed number in order to see the dependence of action as a function of j .

$$\text{Define } X_2 = \begin{pmatrix} x_2 & x_2 \bar{x}_2 \\ I_4 & \bar{x}_2 \end{pmatrix}, V_2 = \begin{pmatrix} a_1 I_4 + a_2 e_1 e_3 & 0 \\ 0 & d_2 e_1 e_3 \end{pmatrix} \text{ and } V_2^\dagger = \begin{pmatrix} d_2 \overline{e_1 e_3} & 0 \\ 0 & a_1 \bar{I}_4 + a_2 \overline{e_1 e_3} \end{pmatrix}.$$

Calculate $V_2 X_2 V_2^\dagger - X_2$.

- 3) Define $\tilde{j}_3 = j_0 + s_3, x_3 = \tilde{j}_1 e_2 e_3 + \tilde{j}_2 e_1 e_3 + \tilde{j}_3 e_1 e_2, \bar{x}_3 = \tilde{j}_1 \overline{e_2 e_3} + \tilde{j}_2 \overline{e_1 e_3} + \tilde{j}_3 \overline{e_1 e_2}$.

$$\text{Define } X_3 = \begin{pmatrix} x_3 & x_3 \bar{x}_3 \\ I_4 & \bar{x}_3 \end{pmatrix}, V_3 = \begin{pmatrix} a_1 I_4 & 0 \\ 0 & d_1 e_2 e_4 \end{pmatrix} \text{ and } V_3^\dagger = \begin{pmatrix} d_1 \overline{e_2 e_4} & 0 \\ 0 & a_1 \bar{I}_4 \end{pmatrix}.$$

Calculate $V_3 X_3 V_3^\dagger - X_3$.

From step 4, the simulation depends on paths. In order to check my program, I first replace ambiguous $e_1 e_4$ and $e_2 e_4$ in $L21$ and $L22$ by $e_3 e_4$. To check my program, I also replace $e_1 e_4$ and $-e_2 e_4$ in $L23$ and $L24$ by $e_3 e_4$ and $-e_3 e_4$, respectively.

5.1 L19

- 4) In the case of $L19$, define $\tilde{j}_4 = j_0 + s_4, x_4 = \tilde{j}_1 e_2 e_3 + \tilde{j}_2 e_1 e_3 + \tilde{j}_3 e_1 e_2 + \tilde{j}_4 e_2 e_4, \bar{x}_4 = \tilde{j}_1 \overline{e_2 e_3} + \tilde{j}_2 \overline{e_1 e_3} + \tilde{j}_3 \overline{e_1 e_2} + \tilde{j}_4 \overline{e_2 e_4}$.

$$\text{Define } X_4 = \begin{pmatrix} x_4 & x_4 \bar{x}_4 \\ I_4 & \bar{x}_4 \end{pmatrix}, V_4 = \begin{pmatrix} a_1 I_4 - a_2 e_1 e_2 & 0 \\ 0 & d_2 e_1 e_2 \end{pmatrix} \text{ and}$$

$$V_4^\dagger = \begin{pmatrix} -d_2 \overline{e_1 e_2} & 0 \\ 0 & a_1 \bar{I}_4 - a_2 \overline{e_1 e_2} \end{pmatrix}$$

Calculate $V_4 X_4 V_4^\dagger - X_4$.

- 5) Define $\tilde{j}_5 = j_0 + s_3, x_5 = \tilde{j}_1 e_2 e_3 + \tilde{j}_2 e_1 e_3 + (\tilde{j}_3 - \tilde{j}_5) e_1 e_2 + \tilde{j}_4 e_2 e_4, \bar{x}_5 = \tilde{j}_1 \overline{e_2 e_3} + \tilde{j}_2 \overline{e_1 e_3} + (\tilde{j}_3 - \tilde{j}_5) \overline{e_1 e_2} + \tilde{j}_4 \overline{e_2 e_4}$.

Define $X_5 = \begin{pmatrix} x_5 & x_5 \bar{x}_5 \\ I_4 & \bar{x}_5 \end{pmatrix}, V_5 = \begin{pmatrix} a_1 I_4 & 0 \\ 0 & -d_1 e_2 e_4 \end{pmatrix}$ and $V_5^\dagger = \begin{pmatrix} -d_1 \overline{e_2 e_4} & 0 \\ 0 & a_1 \bar{I}_4 \end{pmatrix}$

Calculate $V_5 X_5 V_5^\dagger - X_5$.
- 6) Define $\tilde{j}_6 = j_0 + s_4, x_6 = \tilde{j}_1 e_2 e_3 + \tilde{j}_2 e_1 e_3 + (\tilde{j}_3 - \tilde{j}_5) e_1 e_2 + \tilde{j}_4 e_2 e_4, \bar{x}_6 = \tilde{j}_1 \overline{e_2 e_3} + \tilde{j}_2 \overline{e_1 e_3} + (\tilde{j}_3 - \tilde{j}_5) \overline{e_1 e_2} + (\tilde{j}_4 - \tilde{j}_6) \overline{e_2 e_4}$.

Define $X_6 = \begin{pmatrix} x_6 & x_6 \bar{x}_6 \\ I_4 & \bar{x}_6 \end{pmatrix}, V_6 = \begin{pmatrix} a_1 I_4 & -b_1 e_2 e_3 \\ -c_1 e_2 e_3 & 0 \end{pmatrix}$ and $V_6^\dagger = \begin{pmatrix} 0 & -c_1 \overline{e_2 e_3} \\ -b_1 \overline{e_2 e_3} & a_1 \bar{I}_4 \end{pmatrix}$.

Calculate $V_6 X_6 V_6^\dagger - X_6$.
- 7) Define $\tilde{j}_7 = j_0 + s_1, x_7 = (\tilde{j}_1 - \tilde{j}_7) e_2 e_3 + \tilde{j}_2 e_1 e_3 + (\tilde{j}_3 - \tilde{j}_5) e_1 e_2 + \tilde{j}_4 e_2 e_4, \bar{x}_7 = (\tilde{j}_1 - \tilde{j}_7) \overline{e_2 e_3} + \tilde{j}_2 \overline{e_1 e_3} + (\tilde{j}_3 - \tilde{j}_5) \overline{e_1 e_2} + (\tilde{j}_4 - \tilde{j}_6) \overline{e_2 e_4}$.

Define $X_7 = \begin{pmatrix} x_7 & x_7 \bar{x}_7 \\ I_4 & \bar{x}_7 \end{pmatrix}, V_7 = \begin{pmatrix} a_1 I_4 & -b_2 e_1 e_3 \\ -c_2 e_1 e_3 & 0 \end{pmatrix}$ and

$V_7^\dagger = \begin{pmatrix} 0 & -c_2 \overline{e_1 e_3} \\ -b_2 \overline{e_1 e_3} & a_1 \bar{I}_4 \end{pmatrix}$

Calculate $V_7 X_7 V_7^\dagger - X_7$.
- 8) Define $\tilde{j}_8 = j_0 + s_2, x_8 = (\tilde{j}_1 - \tilde{j}_7) e_2 e_3 + (\tilde{j}_2 - \tilde{j}_8) e_1 e_3 + (\tilde{j}_3 - \tilde{j}_5) e_1 e_2 + \tilde{j}_4 e_2 e_4, \bar{x}_8 = (\tilde{j}_1 - \tilde{j}_7) \overline{e_2 e_3} + (\tilde{j}_2 - \tilde{j}_8) \overline{e_1 e_3} + (\tilde{j}_3 - \tilde{j}_5) \overline{e_1 e_2} + (\tilde{j}_4 - \tilde{j}_6) \overline{e_2 e_4}$.

Define $X_8 = \begin{pmatrix} x_8 & x_8 \bar{x}_8 \\ I_4 & \bar{x}_8 \end{pmatrix}, V_8 = \begin{pmatrix} a_1 I_4 & -b_1 e_2 e_3 \\ -c_1 e_2 e_3 & 0 \end{pmatrix}$ and $V_8^\dagger = \begin{pmatrix} 0 & -c_1 \overline{e_2 e_3} \\ -b_1 \overline{e_2 e_3} & a_1 \bar{I}_4 \end{pmatrix}$.

Calculate $V_8 X_8 V_8^\dagger - X_8$.
- 9) In the case of step 3 and step 4, the variance of average of absolute value of eigenvalues are large. The large variance can be reduced by the singular value decomposition (SVD) method[36].

5.2 L20

- 4-5) Same as $L19$

- 6) Define $\tilde{j}_6 = j_0 + s_2, x_6 = (\tilde{j}_1 - \tilde{j}_5)e_2e_3 + (\tilde{j}_2 - \tilde{j}_6)e_1e_3 + \tilde{j}_3e_1e_2 + \tilde{j}_4e_2e_4, \bar{x}_6 = (\tilde{j}_1 - \tilde{j}_5)\overline{e_2e_3} + (\tilde{j}_2 - \tilde{j}_6)\overline{e_1e_3} + \tilde{j}_3\overline{e_1e_2} + \tilde{j}_4\overline{e_2e_4}$.

$$\text{Define } X_6 = \begin{pmatrix} x_6 & x_6\bar{x}_6 \\ I_4 & \bar{x}_6 \end{pmatrix}, V_6 = \begin{pmatrix} a_1I_4 & -b_2e_1e_3 \\ -c_2e_1e_3 & 0 \end{pmatrix} \text{ and } V_6^\dagger = \begin{pmatrix} 0 & -c_2\overline{e_1e_3} \\ -b_2\overline{e_1e_3} & a_1\bar{I}_4 \end{pmatrix}$$

Calculate $V_6X_6V_6^\dagger - X_6$.

- 7) Define $\tilde{j}_7 = j_0 + s_3, x_7 = (\tilde{j}_1 - \tilde{j}_5)e_2e_3 + (\tilde{j}_2 - \tilde{j}_6)e_1e_3 + (\tilde{j}_3 - \tilde{j}_7)e_1e_2 + \tilde{j}_4e_2e_4, \bar{x}_7 = (\tilde{j}_1 - \tilde{j}_5)\overline{e_2e_3} + (\tilde{j}_2 - \tilde{j}_6)\overline{e_1e_3} + (\tilde{j}_3 - \tilde{j}_7)\overline{e_1e_2} + \tilde{j}_4\overline{e_2e_4}$.

$$\text{Define } X_7 = \begin{pmatrix} x_7 & x_7\bar{x}_7 \\ I_4 & \bar{x}_7 \end{pmatrix}, V_7 = \begin{pmatrix} a_1I_4 - a_2e_1e_2 & 0 \\ 0 & -d_2e_1e_2 \end{pmatrix} \text{ and}$$

$$V_7^\dagger = \begin{pmatrix} -d_2\overline{e_1e_2} & 0 \\ 0 & a_1\bar{I}_4 - a_2\overline{e_1e_2} \end{pmatrix}$$

Calculate $V_7X_7V_7^\dagger - X_7$.

- 8) Define $\tilde{j}_8 = j_0 + s_4, x_8 = (\tilde{j}_1 - \tilde{j}_5)e_2e_3 + (\tilde{j}_2 - \tilde{j}_6)e_1e_3 + (\tilde{j}_3 - \tilde{j}_7)e_1e_2 + \tilde{j}_4e_2e_4, \bar{x}_8 = (\tilde{j}_1 - \tilde{j}_5)\overline{e_2e_3} + (\tilde{j}_2 - \tilde{j}_6)\overline{e_1e_3} + (\tilde{j}_3 - \tilde{j}_7)\overline{e_1e_2} + (\tilde{j}_4 - \tilde{j}_8)\overline{e_2e_4}$.

$$\text{Define } X_8 = \begin{pmatrix} x_8 & x_8\bar{x}_8 \\ I_4 & \bar{x}_8 \end{pmatrix}, V_8 = \begin{pmatrix} a_1I_4 & 0 \\ 0 & -d_1e_2e_4 \end{pmatrix} \text{ and } V_8^\dagger = \begin{pmatrix} -d_1\overline{e_2e_4} & 0 \\ 0 & a_1\bar{I}_4 \end{pmatrix}$$

Calculate $V_8X_8V_8^\dagger - X_8$.

5.3 L21

The step 6 is $-e_3e_4$. The step 3 is e_1e_4 or e_2e_4 , but mixing of different e_ke_4 causes mixing of real coordinate and imaginary coordinate. Therefore we double the number of steps and consider $e_1e_4, -e_1e_4$ and $e_2e_4, -e_2e_4$ pairs as shown in Table 2..

- 4) Define $\tilde{j}_4 = j_0 + s_4, x_4 = \tilde{j}_1e_2e_3 + \tilde{j}_2e_1e_3 + \tilde{j}_3e_1e_2 + \tilde{j}_4e_3e_4, \bar{x}_4 = \tilde{j}_1\overline{e_2e_3} + \tilde{j}_2\overline{e_1e_3} + \tilde{j}_3\overline{e_1e_2} + \tilde{j}_4\overline{e_3e_4}$,

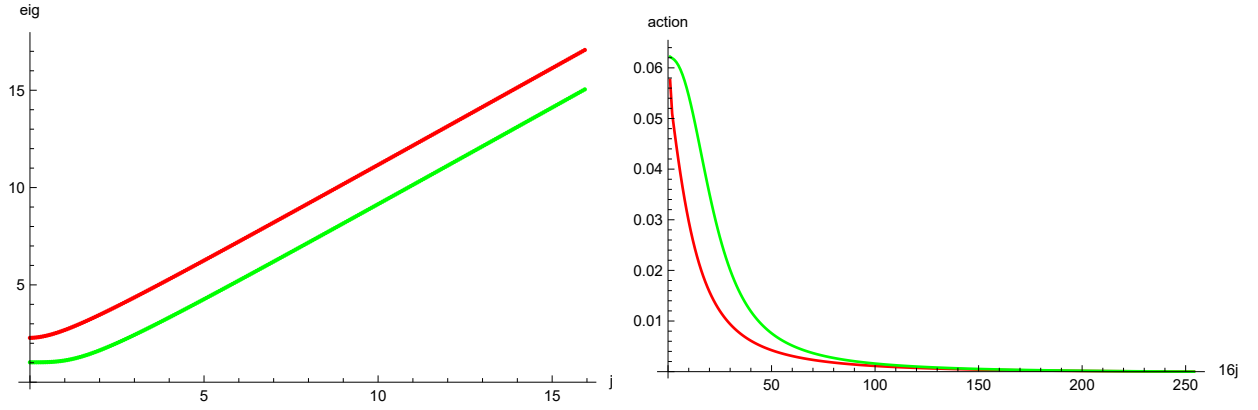


Figure 8: Eigenvalues (left) and actions (right) of L_{19}, L_{20}, L_{25} and L_{21}, L_{22} with $e_2 e_4$ step 3 after Singular Value Decomposition (SVD). Red points are contribution of large eigenvalues, green points are contribution of small eigenvalues. The value j is the coordinate of u_1 . $u_2 = 3$.

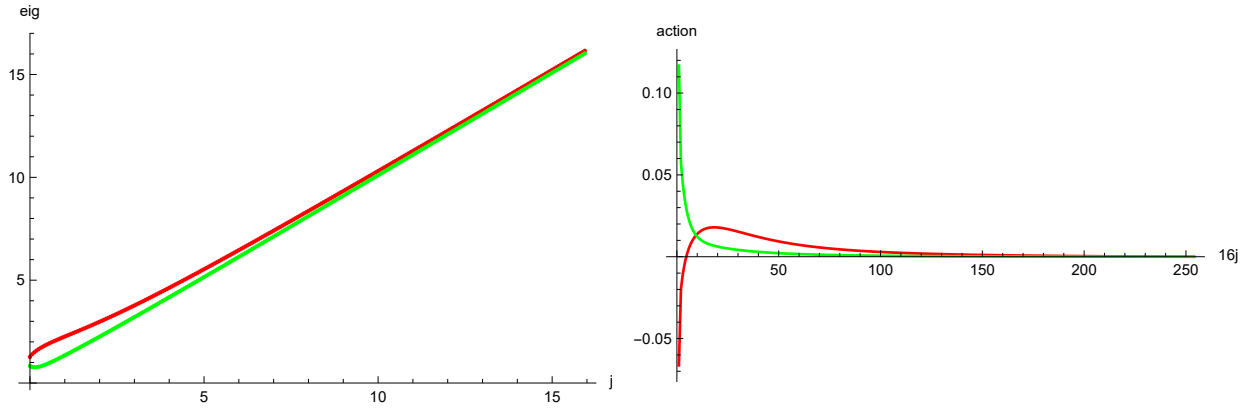


Figure 9: Eigenvalues (left) and actions (right) of L_{23}, L_{24} and L_{21}, L_{22} with $e_1 e_4$ step 3 after SVD. Red lines are the contribution of large eigenvalues, green lines are contribution of small eigenvalues. The value j is the coordinate of u_1 . $u_2 = 1$

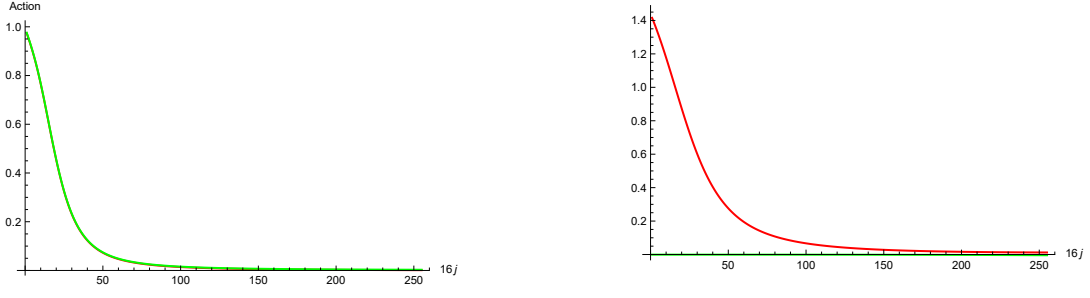


Figure 10: The action of $L22$ step 12 (left) and $L24$ step 10 as a function of $16j = 0, \dots, 255$. Red lines are the contribution of large eigenvalues, green lines are the contribution of small eigenvalues.

$u_2 = 3$

Define $X_4 = \begin{pmatrix} x_4 & x_4 \bar{x}_4 \\ I_4 & \bar{x}_4 \end{pmatrix}$, $V_4 = \begin{pmatrix} a_1 I_4 & 0 \\ 0 & d_1 e_3 e_4 \end{pmatrix}$ and $V_4^\dagger = \begin{pmatrix} d_1 \overline{e_3 e_4} & 0 \\ 0 & a_1 \bar{I}_4 \end{pmatrix}$

Calculate $V_4 X_4 V_4^\dagger - X_4$.

- 5) Same as $L19$.
- 6) Same as $L19$.
- 7) Define $\tilde{j}_7 = j_0 + s_4$, $x_7 = (\tilde{j}_1 - \tilde{j}_6)e_2 e_3 + \tilde{j}_2 e_1 e_3 + (\tilde{j}_3 - \tilde{j}_5)e_1 e_2 + (\tilde{j}_4 - \tilde{j}_7)e_3 e_4$, $\bar{x}_4 = (\tilde{j}_1 - \tilde{j}_6)\overline{e_2 e_3} + \tilde{j}_2 \overline{e_1 e_3} + (\tilde{j}_3 - \tilde{j}_5)\overline{e_1 e_2} + (\tilde{j}_4 - \tilde{j}_7)\overline{e_3 e_4}$,

Define $X_7 = \begin{pmatrix} x_7 & x_7 \bar{x}_7 \\ I_4 & \bar{x}_7 \end{pmatrix}$, $V_7 = \begin{pmatrix} a_1 I_4 & 0 \\ 0 & -d_1 e_3 e_4 \end{pmatrix}$ and $V_7^\dagger = \begin{pmatrix} -d_1 \overline{e_3 e_4} & 0 \\ 0 & a_1 \bar{I}_4 \end{pmatrix}$

Calculate $V_7 X_7 V_7^\dagger - X_7$.

- 8) Define $\tilde{j}_8 = j_0 + s_2$, $x_8 = (\tilde{j}_1 - \tilde{j}_6)e_2 e_3 + (\tilde{j}_2 - \tilde{j}_8)e_1 e_3 + (\tilde{j}_3 - \tilde{j}_5)e_1 e_2 + (\tilde{j}_4 - \tilde{j}_7)e_3 e_4$, $\bar{x}_4 = (\tilde{j}_1 - \tilde{j}_6)\overline{e_2 e_3} + (\tilde{j}_2 - \tilde{j}_8)\overline{e_1 e_3} + (\tilde{j}_3 - \tilde{j}_5)\overline{e_1 e_2} + (\tilde{j}_4 - \tilde{j}_7)\overline{e_3 e_4}$,

Define $X_8 = \begin{pmatrix} x_8 & x_8 \bar{x}_8 \\ I_4 & \bar{x}_8 \end{pmatrix}$, $V_8 = \begin{pmatrix} a_1 I_4 & -b_2 e_1 e_3 \\ -c_2 e_1 e_3 & 0 \end{pmatrix}$ and $V_8^\dagger = \begin{pmatrix} 0 & -c_2 \overline{e_1 e_3} \\ -b_2 \overline{e_1 e_3} & a_1 \bar{I}_4 \end{pmatrix}$

Calculate $V_8 X_8 V_8^\dagger - X_8$.

5.4 L22

- 4) In the step 3, there are two possibilities e_1e_4 or e_2e_4 . The latter is same as $L19$ and the former is same as $L21$.
- 5) The step 4 is same as $L19$ and $L21$
- 6) Define $\tilde{j}_6 = j_0 + s_1$,

$$x_6 = (\tilde{j}_1 - \tilde{j}_6)e_2e_3 + \tilde{j}_2e_1e_3 + (\tilde{j}_3 - \tilde{j}_5)e_1e_2 + \tilde{j}_4e_2e_4, \bar{x}_6 = (\tilde{j}_1 - \tilde{j}_6)\overline{e_2e_3} + \tilde{j}_2\overline{e_1e_3} + (\tilde{j}_3 - \tilde{j}_5)\overline{e_1e_2} + \tilde{j}_4\overline{e_2e_4}.$$

$$x_6 = (\tilde{j}_1 - \tilde{j}_6)e_2e_3 + \tilde{j}_2e_1e_3 + (\tilde{j}_3 - \tilde{j}_5)e_1e_2 + \tilde{j}_4e_1e_4, \bar{x}_6 = (\tilde{j}_1 - \tilde{j}_6)\overline{e_2e_3} + \tilde{j}_2\overline{e_1e_3} + (\tilde{j}_3 - \tilde{j}_5)\overline{e_1e_2} + \tilde{j}_4\overline{e_1e_4}$$

$$\text{Define } X_6 = \begin{pmatrix} x_6 & x_6\bar{x}_6 \\ I_4 & \bar{x}_6 \end{pmatrix}, V_6 = \begin{pmatrix} a_1I_4 & -b_1e_2e_3 \\ -c_1e_2e_3 & 0 \end{pmatrix} \text{ and } V_6^\dagger = \begin{pmatrix} 0 & -c_1\overline{e_2e_3} \\ -b_1\overline{e_2e_3} & a_1\bar{I}_4 \end{pmatrix}.$$

Calculate $V_6X_6V_6^\dagger - X_6$.

- 7) Define $\tilde{j}_7 = j_0 + s_2$,

$$x_7 = (\tilde{j}_1 - \tilde{j}_6)e_2e_3 + (\tilde{j}_2 - \tilde{j}_7)e_1e_3 + (\tilde{j}_3 - \tilde{j}_5)e_1e_2 + \tilde{j}_4e_2e_4, \bar{x}_7 = (\tilde{j}_1 - \tilde{j}_6)\overline{e_2e_3} + \tilde{j}_2\overline{e_1e_3} + (\tilde{j}_3 - \tilde{j}_5)\overline{e_1e_2} + \tilde{j}_4\overline{e_2e_4}.$$

$$x_7 = (\tilde{j}_1 - \tilde{j}_6)e_2e_3 + (\tilde{j}_2 - \tilde{j}_7)e_1e_3 + (\tilde{j}_3 - \tilde{j}_5)e_1e_2 + \tilde{j}_4e_1e_4, \bar{x}_7 = (\tilde{j}_1 - \tilde{j}_6)\overline{e_2e_3} + (\tilde{j}_2 - \tilde{j}_7)\overline{e_1e_3} + (\tilde{j}_3 - \tilde{j}_5)\overline{e_1e_2} + \tilde{j}_4\overline{e_1e_4}$$

$$\text{Define } X_7 = \begin{pmatrix} x_7 & x_7\bar{x}_7 \\ I_4 & \bar{x}_7 \end{pmatrix}, V_7 = \begin{pmatrix} a_1I_4 & -b_2e_1e_3 \\ -c_2e_1e_3 & 0 \end{pmatrix} \text{ and } V_7^\dagger = \begin{pmatrix} 0 & -c_2\overline{e_1e_3} \\ -b_2\overline{e_1e_3} & a_1\bar{I}_4 \end{pmatrix}$$

Calculate $V_7X_7V_7^\dagger - X_7$.

- 8) Define $j_8 = j_0 + s_4$. $x_8 = (\tilde{j}_1 - \tilde{j}_6)e_2e_3 + (\tilde{j}_2 - \tilde{j}_7)e_1e_3 + (\tilde{j}_3 - \tilde{j}_5)e_1e_2 + \tilde{j}_4e_2e_4 - \tilde{j}_8e_3e_4$,
 $\bar{x}_8 = (\tilde{j}_1 - \tilde{j}_6)\overline{e_2e_3} + \tilde{j}_2\overline{e_1e_3} + (\tilde{j}_3 - \tilde{j}_5)\overline{e_1e_2} + \tilde{j}_4\overline{e_2e_4} - \tilde{j}_8\overline{e_3e_4}.$

$$\text{Define } X_8 = \begin{pmatrix} x_8 & x_8\bar{x}_8 \\ I_4 & \bar{x}_8 \end{pmatrix}, V_8 = \begin{pmatrix} a_1I_4 & 0 \\ 0 & -d_1e_3e_4 \end{pmatrix} \text{ and } V_8^\dagger = \begin{pmatrix} d_1\overline{e_3e_4} & 0 \\ 0 & a_1\bar{I}_4 \end{pmatrix}$$

Calculate $V_8X_8V_8^\dagger - X_8$.

5.5 L23

- 4) The step 3 is e_1e_4 but the step 6 is $-e_2e_4$. We double the number of steps as shown in the Table 2.

- 5) Define $\tilde{j}_5 = j_0 + s_2$,

$$x_5 = \tilde{j}_1e_2e_3 + (\tilde{j}_2 - \tilde{j}_5)e_1e_3 + \tilde{j}_3e_1e_2 + \tilde{j}_4e_2e_4, \bar{x}_5 = \tilde{j}_1\overline{e_2e_3} + (\tilde{j}_2 - \tilde{j}_5)\overline{e_1e_3} + \tilde{j}_3\overline{e_1e_2} + \tilde{j}_4\overline{e_3e_4}.$$

- 6) Define $\tilde{j}_6 = j_0 + s_1$, $x_6 = (\tilde{j}_1 - \tilde{j}_6)e_2e_3 + (\tilde{j}_2 - \tilde{j}_5)e_1e_3 + \tilde{j}_3e_1e_2 + \tilde{j}_4e_1e_4$, $\bar{x}_5 = (\tilde{j}_1 - \tilde{j}_6)\overline{e_2e_3} + \tilde{j}_2\overline{e_1e_3} + (\tilde{j}_3 - \tilde{j}_5)\overline{e_1e_2} + \tilde{j}_4\overline{e_3e_4}$

$$\text{Define } X_6 = \begin{pmatrix} x_6 & x_6\bar{x}_6 \\ I_4 & \bar{x}_6 \end{pmatrix}, V_6 = \begin{pmatrix} a_1I_4 & -b_2e_1e_3 \\ -c_2e_1e_3 & 0 \end{pmatrix} \text{ and } V_6^\dagger = \begin{pmatrix} 0 & -c_2\overline{e_1e_3} \\ -b_2\overline{e_1e_3} & a_1\bar{I}_4 \end{pmatrix}.$$

Calculate $V_6X_6V_6^\dagger - X_6$.

- 7) Define $\tilde{j}_7 = j_0 + s_4$, $x_7 = (\tilde{j}_1 - \tilde{j}_6)e_2e_3 + (\tilde{j}_2 - \tilde{j}_5)e_1e_3 + \tilde{j}_3e_1e_2 + \tilde{j}_4e_1e_4$, $\bar{x}_7 = (\tilde{j}_1 - \tilde{j}_6)\overline{e_2e_3} + \tilde{j}_2\overline{e_1e_3} + \tilde{j}_3\overline{e_1e_2} + (\tilde{j}_4 - \tilde{j}_7)\overline{e_3e_4}$

$$\text{Define } X_7 = \begin{pmatrix} x_7 & x_7\bar{x}_7 \\ I_4 & \bar{x}_7 \end{pmatrix}, V_7 = \begin{pmatrix} a_1I_4 & 0 \\ 0 & -d_1e_3e_4 \end{pmatrix} \text{ and } V_7^\dagger = \begin{pmatrix} -d_1\overline{e_3e_4} & 0 \\ 0 & a_1\bar{I}_4 \end{pmatrix}.$$

Calculate $V_7X_7V_7^\dagger - X_7$.

- 8) Define $\tilde{j}_8 = j_0 + s_3$, $x_8 = (\tilde{j}_1 - \tilde{j}_6)e_2e_3 + (\tilde{j}_2 - \tilde{j}_5)e_1e_3 + (\tilde{j}_3 - \tilde{j}_8)e_1e_2 + (\tilde{j}_4 - \tilde{j}_7)e_3e_4$, $\bar{x}_8 = (\tilde{j}_1 - \tilde{j}_6)\overline{e_2e_3} + \tilde{j}_2\overline{e_1e_3} + (\tilde{j}_3 - \tilde{j}_8)\overline{e_1e_2} + (\tilde{j}_4 - \tilde{j}_7)\overline{e_3e_4}$.

$$\text{Define } X_8 = \begin{pmatrix} x_8 & x_8\bar{x}_8 \\ I_4 & \bar{x}_8 \end{pmatrix}, V_8 = \begin{pmatrix} a_1I_4 - a_2e_1e_2 & 0 \\ 0 & -d_2e_1e_2 \end{pmatrix} \text{ and } V_8^\dagger = \begin{pmatrix} -d_2\overline{e_1e_2} & 0 \\ 0 & a_1\bar{I}_4 - a_2\overline{e_1e_2} \end{pmatrix}.$$

Calculate $V_8X_8V_8^\dagger - X_8$.

5.6 L24

Up to the step 5 $L24 = L23$.

- 7) Define $\tilde{j}_7 = j_0 + s_3$, $x_7 = (\tilde{j}_1 - \tilde{j}_6)e_2e_3 + (\tilde{j}_2 - \tilde{j}_5)e_1e_3 + (\tilde{j}_3 - \tilde{j}_7)e_1e_2 + \tilde{j}_4e_3e_4$, $\bar{x}_7 = (\tilde{j}_1 - \tilde{j}_6)\overline{e_2e_3} + \tilde{j}_2\overline{e_1e_3} + (\tilde{j}_3 - \tilde{j}_7)\overline{e_1e_2} + \tilde{j}_4\overline{e_3e_4}$

Define $X_7 = \begin{pmatrix} x_7 & x_7\bar{x}_7 \\ I_4 & \bar{x}_7 \end{pmatrix}$, $V_7 = \begin{pmatrix} a_1I_4 - a_2e_1e_2 & 0 \\ 0 & -d_2e_1e_2 \end{pmatrix}$ and

$$V_7^\dagger = \begin{pmatrix} -d_2\overline{e_1e_2} & 0 \\ 0 & a_1\bar{I}_4 - a_2\overline{e_1e_2} \end{pmatrix}.$$

Calculate $V_7X_7V_7^\dagger - X_7$.

- 8) Define $\tilde{j}_8 = j_0 + s_4$, $x_8 = (\tilde{j}_1 - \tilde{j}_6)e_2e_3 + (\tilde{j}_2 - \tilde{j}_5)e_1e_3 + (\tilde{j}_3 - \tilde{j}_7)e_1e_2 + (\tilde{j}_4 - \tilde{j}_8)e_3e_4$, $\bar{x}_8 = (\tilde{j}_1 - \tilde{j}_6)\overline{e_2e_3} + \tilde{j}_2\overline{e_1e_3} + (\tilde{j}_3 - \tilde{j}_7)\overline{e_1e_2} + (\tilde{j}_4 - \tilde{j}_8)\overline{e_3e_4}$

Define $X_8 = \begin{pmatrix} x_8 & x_8\bar{x}_8 \\ I_4 & \bar{x}_8 \end{pmatrix}$, $V_8 = \begin{pmatrix} a_1I_4 & 0 \\ 0 & -d_1e_3e_4 \end{pmatrix}$ and $V_8^\dagger = \begin{pmatrix} -d_1\overline{e_3e_4} & 0 \\ 0 & a_1\bar{I}_4 \end{pmatrix}$.

Calculate $V_8X_8V_8^\dagger - X_8$.

5.7 L25

- 4) The step 3 of $L25$ is along e_2e_4 and the step 6 is along $-e_2e_4$. The transformations are same as $L19$.

- 5) Define $\tilde{j}_5 = j_0 + s_1$, $x_5 = (\tilde{j}_1 - \tilde{j}_5)e_2e_3 + \tilde{j}_2e_1e_3 + \tilde{j}_3e_1e_2 + \tilde{j}_4e_2e_4$, $\bar{x}_5 = (\tilde{j}_1 - \tilde{j}_5)\overline{e_2e_3} + \tilde{j}_2\overline{e_1e_3} + \tilde{j}_3\overline{e_1e_2} + \tilde{j}_4\overline{e_2e_4}$.

Define $X_5 = \begin{pmatrix} x_5 & x_5\bar{x}_5 \\ I_4 & \bar{x}_5 \end{pmatrix}$, $V_5 = \begin{pmatrix} a_1I_4 & -b_1e_2e_3 \\ -c_1e_2e_3 & 0 \end{pmatrix}$ and

$$V_5^\dagger = \begin{pmatrix} 0 & -c_1\overline{e_2e_3} \\ -b_1\overline{e_2e_3} & a_1\bar{I}_4 \end{pmatrix}$$

Calculate $V_5X_5V_5^\dagger - X_5$.

- 6) Define $\tilde{j}_6 = j_0 + s_2$, $x_6 = (\tilde{j}_1 - \tilde{j}_5)e_2e_3 + (\tilde{j}_2 - \tilde{j}_6)e_1e_3 + \tilde{j}_3e_1e_2 + \tilde{j}_4e_2e_4$, $\bar{x}_6 = (\tilde{j}_1 - \tilde{j}_5)\overline{e_2e_3} + (\tilde{j}_2 - \tilde{j}_6)\overline{e_1e_3} + \tilde{j}_3\overline{e_1e_2} + \tilde{j}_4\overline{e_2e_4}$.

Define $X_6 = \begin{pmatrix} x_6 & x_6\bar{x}_6 \\ I_4 & \bar{x}_6 \end{pmatrix}$, $V_6 = \begin{pmatrix} a_1I_4 & -b_2e_1e_3 \\ -c_2e_1e_3 & 0 \end{pmatrix}$ and $V_6^\dagger = \begin{pmatrix} 0 & -c_2\overline{e_1e_3} \\ -b_2\overline{e_1e_3} & a_1\bar{I}_4 \end{pmatrix}$

Calculate $V_6 X_6 V_6^\dagger - X_6$.

- 7) Define $\tilde{j}_7 = j_0 + s_3, x_7 = (\tilde{j}_1 - \tilde{j}_5)e_2e_3 + (\tilde{j}_2 - \tilde{j}_6)e_1e_3 + (\tilde{j}_3 - \tilde{j}_7)e_1e_2 + \tilde{j}_4e_2e_4, \bar{x}_7 = (\tilde{j}_1 - \tilde{j}_5)\overline{e_2e_3} + (\tilde{j}_2 - \tilde{j}_6)\overline{e_1e_3} + \tilde{j}_3\overline{e_1e_2} + \tilde{j}_4\overline{e_2e_4}$.

$$\text{Define } X_7 = \begin{pmatrix} x_7 & x_7\bar{x}_7 \\ I_4 & \bar{x}_7 \end{pmatrix}, V_7 = \begin{pmatrix} a_1I_4 - a_2e_1e_2 & 0 \\ 0 & -d_2e_1e_2 \end{pmatrix} \text{ and } V_7^\dagger = \begin{pmatrix} -d_2\overline{e_1e_2} & 0 \\ 0 & a_1\bar{I}_4 - a_2\overline{e_1e_2} \end{pmatrix}$$

Calculate $V_7 X_7 V_7^\dagger - X_7$.

- 8) Define $\tilde{j}_8 = j_0 + s_4, x_8 = (\tilde{j}_1 - \tilde{j}_5)e_2e_3 + (\tilde{j}_2 - \tilde{j}_6)e_1e_3 + (\tilde{j}_3 - \tilde{j}_7)e_1e_2 + (\tilde{j}_4 - \tilde{j}_8)e_2e_4, \bar{x}_8 = (\tilde{j}_1 - \tilde{j}_5)\overline{e_2e_3} + (\tilde{j}_2 - \tilde{j}_6)\overline{e_1e_3} + \tilde{j}_3\overline{e_1e_2} + (\tilde{j}_4 - \tilde{j}_8)\overline{e_2e_4}$.

$$\text{Define } X_8 = \begin{pmatrix} x_8 & x_8\bar{x}_8 \\ I_4 & \bar{x}_8 \end{pmatrix}, V_8 = \begin{pmatrix} a_1I_4 & 0 \\ 0 & -d_1e_2e_4 \end{pmatrix} \text{ and } V_8^\dagger = \begin{pmatrix} -d_1\overline{e_2e_4} & 0 \\ 0 & a_1\bar{I}_4 \end{pmatrix}$$

Calculate $V_8 X_8 V_8^\dagger - X_8$.

5.8 Numerical Results

I calculated the average of absolute value of eigenvalues of $X\bar{X}$ for time transformation proportional to e_2e_4 ($L19, L20, L25$) and to e_1e_4 ($L21, L22, L23, L24$) at the step 3. I checked that the absolute values of the eigenvalue of $x\bar{x}$ in \mathcal{X} have a peak in the middle of steps and vanish at the step 8 and the eigenvalues of the ($L19, L20, L25$) agree, and those of ($L21, L22, L23, L24$) agree.

The method of SVD was applied in the tensor renormalization [37, 38, 39, 41]. A package for Grassmann tensor network written in Python [40] is used in a spacial 2D, flavor 3D QCD simulation[41], and the simplicity of their algorithm as compared to [37, 38, 39] was remarked. But I guess that the simplicity is due to the fact that the spacial dimension is two.

One quaternion in $(3+1)D$ simulation is represented by a 4×4 matrix, and there are 4 eigenvalues. In some loops like $L21$, they are nearly equal but in some loops like $L19, L20, L24$ there are 2 kinds of eigenvalues and we need to separate the two groups, in order to reduce the variance.

5.9 Hysteresis effects

Mathematica is a powerfull tool to study quaternions. In [42] a formula

$$\exp A[\mathbf{x}] = I + \frac{\sin \ell}{\ell} A[\mathbf{x}] + \frac{1 - \cos \ell}{\ell^2} A[\mathbf{x}]^2 \quad (60)$$

where $A[\mathbf{x}] = \begin{pmatrix} 0 & -z & y \\ z & 0 & -x \\ -y & x & 0 \end{pmatrix}$ satisfies $A[\mathbf{x}]\mathbf{w} = \mathbf{x} \times \mathbf{w}$ for all $\mathbf{w} \in R^3$ is derived using quaternions.

In $(2+1)D$, quaternions $\mathbf{q}_1 = a_1 + b_1\mathbf{i}$, $\mathbf{q}_2 = a_2 + b_2\mathbf{j}$ satisfy $\mathbf{q}_1\mathbf{q}_2 = a_1a_2 + b_1a_2\mathbf{i} + a_1b_2\mathbf{j} + b_1b_2\mathbf{k}$.

The matrix of the rotation around \mathbf{x} with a counterclockwise angle $|\mathbf{x}| = \ell$ equals

$$R[\mathbf{x}] = \begin{pmatrix} 1 & 0 & 0 \\ 0 & 1 & f_{23}(\ell) \\ 0 & f_{32}(\ell) & 1 \end{pmatrix} \quad (61)$$

The $f_{23}(\ell)$ and the $f_{32}(\ell)$ are shown in Fig.12. Evaluation of the action along the path is not easy, but return to the original point can be seen by the fact that $f_{23}(\ell)$ and $f_{32}(\ell)$ forms a closed curve. The time reversal symmetry in the TR-NEWS will allow derivation of the weight function of $L19 - L25$ from actions obtained after the SVD.

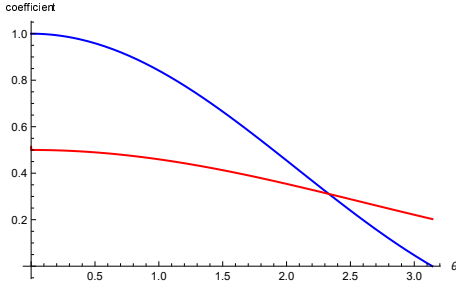


Figure 11: The first coefficient (blue) and the second coefficient (red) of $\exp A[\mathbf{x}]$ as functions of $\theta = |\mathbf{x}|$.

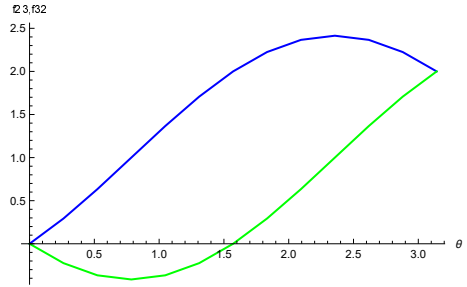


Figure 12: f_{23} (green) and f_{32} (blue) as a function of $\ell = \theta$.

Identifying θ as the time in a frame, the diagram shows hysteresis effects.

Concerning the action of $L19 - L25$, typical data of $L22$ and $L24$ are shown in Fig. 10. The peak of action of $L24$ step 10, whose contribution of smaller eigenvalue part is negligible about

$\sqrt{2}$ times larger than that of $L22$ step 12, whose smaller eigenvalues and the larger eigenvalue are almost degenerate.

In the case of $L19, L20$ and $L25$, actions calculated by the 1st derivative of eigenvalues with respect to the distance from the origin j at steps 6, 7 are 0. In the case of $L21, L22, L23$ and $L24$, actions of steps 5,6,7 and steps 13,14,15 are 0.

It is necessary to calculate the convolution of direct wave and the TR wave that propagate from a position of the transducer to the receiver.

5.10 Rotations in (2+1)D

We applied the same method of calculating action of B type loops in (2+1)D.

step	0	1	2	3	4	5	6	7	8	9	10	11
L3'	x	y	t	-y	-x	-t	x	y	-t	y	x	t
	23	31	34/14	-31	-23	-24	-23	-31	-34/14	31	23	24
L4'	x	y	t	-x	-y	-t						
	23	31	34	-23	-13	-34						
L7'	x	y	x	t	-y	-x	-x	-t				
	23	31	23	34	-13	-23	-23	-34				

Table 3. Directions of the wave front of loops $L3', L4'$ and $L7'$ (z in [34] is replaced by t) the (2+1)D space. In the e_1, e_2, e_4 bases (the first line) and in the $e_i e_j$ bases (the second line).

In these cases, 4 eigenvalues are almost degenerate and the SVD is unnecessary. The link orthogonal to $e_1 \wedge e_2$ is chosen to be $e_1 e_2$.

When $e_1 e_4$ is changed to $e_3 e_4$ in $L3'$, the eigenvalues become similar to those of $L21$. After shifting the time axis, the sum of large eigenvalue and the small eigenvalue at a fixed j becomes 0. Hence action becomes 0.

Since the step 2 of $L4'$ and the step 3 of $L7'$ are restricted to $e_3 e_4$, the derivative of eigenvalues as a function of j is almost constant and there are no action. Absolute value of eigenvalues of $L7'$ is about twice of $L3'$, since $L7'$ contains the path along x axis twice as long as that of $L3'$.

6 Perspective of quaternion quantum field theory

Starting from the extension of the quadratic phase Fourier transform of complex number space of Castro et al.[2] to quaternion number space proposed by Hitzer[1], we presented that the product of quaternions have scalar part and wedge-product parts, and the Dirac's delta function in complex number space cannot be extended to that in quaternion number space as pointed out by Adler in 1985[6].

We extended the mapping of vectors in R^2 space to $R^{2,1}$ space[16, 27, 28] using Clifford algebra bases $e_1, e_2, e_1 \wedge e_2$ done by Porteous[22], to mapping vectors in R^3 space to $R^{3,1}$ space, using bases $e_2e_3, e_3e_1, e_1e_2, e_1e_4, e_2e_4, e_3e_4$ and $\overline{e_2e_3}, \overline{e_3e_1}, \overline{e_1e_2}, \overline{e_1e_4}, \overline{e_2e_4}, \overline{e_3e_4}$.

Porteous obtained actions by sandwiching a state vector of $\mathcal{A}_{2,1}$ expressed by quaternions by Vahlen matrices, which are 2×2 complex matrices. I extended the state vector to that of $\mathcal{A}_{3,1}$ and adopted Clifford bases given by a product of quaternions, which are 4×4 matrices. Proper actions could be obtained by calculating the difference between the transformed vector and the original vector after singular value decompositions.

The standard Dirac equation is[24]

$$D_{3,1}\psi = -\gamma_0 \frac{\partial \psi}{\partial t} + \gamma_1 \frac{\partial \psi}{\partial x_1} + \gamma_2 \frac{\partial \psi}{\partial x_2} + \gamma_3 \frac{\partial \psi}{\partial x_3}, \quad (62)$$

where

$$\begin{aligned} \gamma_0 &= \begin{pmatrix} 0 & I \\ 1 & 0 \end{pmatrix}, \quad \gamma_1 = \begin{pmatrix} 0 & -Q \\ Q & 0 \end{pmatrix}, \\ \gamma_2 &= \begin{pmatrix} 0 & -\sqrt{-1}J \\ \sqrt{-1}J & 0 \end{pmatrix}, \quad \gamma_3 = \begin{pmatrix} 0 & -U \\ U & 0 \end{pmatrix} \end{aligned} \quad (63)$$

In QED, the Lagrangian is

$$\mathcal{L}_{QED} = \sqrt{-1}\bar{\psi}\gamma_\mu(\partial_\mu\psi(x) - \sqrt{-1}eA_\mu(x)\psi(x)) - m\bar{\psi}(x)\psi(x) \quad (64)$$

is invariant under

$$\psi(x) \rightarrow e^{+\sqrt{-1}e\Lambda(x)}\psi(x) \quad (65)$$

$$\bar{\psi}(x) \rightarrow e^{-\sqrt{-1}e\Lambda(x)}\bar{\psi}(x) \quad (66)$$

$$A^\mu(x) \rightarrow A^\mu(x) + \partial^\mu\Lambda(x). \quad (67)$$

Replacement of the Dirac $\gamma(e_i)$ to $\gamma(e_i e_j)$ and to choose proper gauge transformations remains a problem.

Another problem related to NDT is incorporation of the time dependence, or hysteresis effects which can be simulated by the Preisach-Mayergoyz model[30].

Cartan [7] showed in $\nu = 3$ Euclidean space, four sets of 3 vectors can be represented by a linear combination of two products of spinors having quaternion bases, and in $\nu = 4$ Euclidean space, two sets of 4 vectors are coupled to a linear sets of four products of spinors having quaternion bases to form invariants. Adler [6] presented condition for constructing quaternion quantum field theory, and the $\nu = 3$ and $\nu = 4$ case match the condition.

We considered 7 FP actions of DeGrand et al[34] in $R^{3,1}$ lattice space. The rule of continuation of the direction vector of wave fronts in space-time, we found 12 links containing $\pm e_1 e_4$ or $\pm e_2 e_4$ and 2 links containing $-e_3 e_4$.

6.1 Quaternion Fourier Transform and Quaternion Domain Fourier Transform

Hitzer and Sangwine[3] expressed a quaternion q as

$$\begin{aligned} q &= q_r + q_i \mathbf{i} + q_j \mathbf{j} + q_k \mathbf{k} = q_r + \sqrt{q_i^2 + q_j^2 + q_k^2} \mu(q) \\ &= \cos \alpha + \mu(q) \sin \alpha = e^{\alpha \mu(q)} \end{aligned} \quad (68)$$

where $\mu(q) = \frac{q_i \mathbf{i} + q_j \mathbf{j} + q_k \mathbf{k}}{\sqrt{q_i^2 + q_j^2 + q_k^2}}$, $\cos \alpha = q_r$ and $\sin \alpha = \sqrt{q_i^2 + q_j^2 + q_k^2}$. Orthogonal 2D planes split is

$$q_{\pm} = \{q_r \pm q_k + \mathbf{i}(q_i \mp q_j)\} \frac{1 \pm \mathbf{k}}{2} = \frac{1 \pm \mathbf{k}}{2} \{q_r \pm r_k + \mathbf{j}(q_j \mp q_i)\}. \quad (69)$$

Quaternion Fourier transform of a function $h \in L^1(R^2, \mathbf{H})$ described by pure quaternions f, g is

$$\mathcal{F}^{f,g}\{h\}(\omega) = \int_{R^2} e^{-f x_1 \omega_1} h(x) e^{-g x_2 \omega_2} dx_1 dx_2 \quad (70)$$

The method was extended to quaternion valued quaternion domain Fourier transform (QDFT)[17] and applied to an extension of quadratic phase Fourier transform of [2] in the recent article as Quadratic-Phase Quaternion Domain Fourier Transform (QPQDFT)[1].

In the textbook[4] the space-time algebra $Cl_{3,1}$ of Minkowski space $R^{3,1}$ with bases $\{e_1, e_2, e_3, e_t\}$ which have the relation $e_1^2 = e_2^2 = e_3^2 = -e_t^2 = 1$ isomorphic to a system with bases $\{1, e_t, i_3, i_{st}\}$

where

$$i_3 = e_1 e_2 e_3 = e_t^* = e_t i_3^{-1}, \quad i_{st} = e_t i_3, \quad i_{st}^2 = -1, \quad (71)$$

was introduced.

Hitzer defined the volume-time Fourier transform

$$\mathcal{F}_{VT}(\omega) = \int_{R^{3,1}} e^{-e_t \omega_t} h(\mathbf{x}) e^{-\vec{x} \cdot \vec{\omega}} d^4 x \quad (72)$$

where

$$\begin{aligned} \mathbf{x} &= t e_t + \vec{x}, \quad \vec{x} = x_1 e_1 + x_2 e_2 + x_3 e_3, \\ \omega &= \omega_t e_t + \vec{\omega}, \quad \vec{\omega} = \omega_1 e_1 + \omega_2 e_2 + \omega_3 e_3 \end{aligned} \quad (73)$$

The bases of $\mathcal{A}_{3,1}^+$ taken by Garling[24] are

$$e_1 e_3, e_2 e_4, e_1 e_4, e_2 e_3, e_3 e_4, e_1 e_2, e_\Omega, \quad (74)$$

and the bases $e_i e_4$ and $e_j e_4$ ($i \neq j$) do not commute, in contrast to Hitzer's e_t in his volume-time Clifford Fourier transform.

In order to calculate actions in quaternion field theory in $R^{3,1}$, it is necessary to consider the system is isomorphic to $M_2(\mathbf{H})$. The biquaternion space was excluded in Ariel's approach[8, 9].

6.2 Application of (3+1)D quaternion Fourier transform

The (3+1)D quaternion Fourier transform allow 3D image analysis. In present NDT technology, essentially (2+1)D images are analized, but using two quaternion bases $e_i e_j$ and $\overline{e_i e_j}$, three dimensional detection of the scattering position of ultrasonic waves may become possible. In the fixed point action analysis, we found that variance of actions along $e_i e_4$ becomes large, but via the SVD we can decomose the large eigenvalue component and the small eigenvalue component. Recent NDT experiment using water tanks is presented in [31].

Felsberg and Sommer[13] defined in the Riesz wavelet transform of $(2+1)D$

$$G_M(\mathbf{u}) = G_3(u_1, u_2, 0) - \mathbf{i} G_1(u_1, u_2, 0) - \mathbf{j} G_2(u_1, u_2, 0), \quad (75)$$

and applied the Radon transform in R^3 by choosing a hyper plane $\xi(\omega, p) = \{x \in R^3 \mid (x, \omega) = p\}$, where $\omega = (\lambda_1, \lambda_2, \lambda_3)$ is a unit vector, $(x, \omega) = \sum_i x_i \lambda_i$.

For a function $f \in R^3$, $\hat{f}(\xi) = \hat{f}(\xi, p) = \int_{\xi} f(x) d_{\xi} x$ is called the Fourier transform on Radon measure or Radon transform [44, 45, 46]. Here, $d_{\xi} x \wedge d\omega = dx$ is the volume element.

We define

$$\begin{aligned} G_{M1}(\mathbf{u}) &= G_0(\mathbf{u}) - e_2 e_3 G_{23}(\mathbf{u}) - e_1 e_3 G_{13}(\mathbf{u}) - e_1 e_2 G_{12}(\mathbf{u}) - e_1 e_4 G_{14}(\mathbf{u}) \\ G_{M2}(\mathbf{u}) &= G_0(\mathbf{u}) - e_2 e_3 G_{23}(\mathbf{u}) - e_1 e_3 G_{13}(\mathbf{u}) - e_1 e_2 G_{12}(\mathbf{u}) - e_2 e_4 G_{24}(\mathbf{u}) \\ G_{M3}(\mathbf{u}) &= G_0(\mathbf{u}) - e_2 e_3 G_{23}(\mathbf{u}) - e_1 e_3 G_{13}(\mathbf{u}) - e_1 e_2 G_{12}(\mathbf{u}) - e_3 e_4 G_{34}(\mathbf{u}). \end{aligned} \quad (76)$$

By defining the space of hyperplanes as \mathcal{F} , the Plancherel's formula says [44, 46]

$$F_M = \int_M |f(x)|^2 dx = \int_{\mathcal{F}} |\wedge \hat{f}(\xi)|^2 d\xi. \quad (77)$$

where $f(x) = \frac{dF}{dx}$ is unique, when F_M is additive. For complex valued function in L^2 space the formula is established [35], but for quaternion valued functions $M_2(\mathbf{H})$, it is not.

Since numerical results suggest that $F_{M3} \neq F_{M1} = F_{M2}$, the topology of M_3 is different from that of M_1 and M_2 . In (2+1)D QED [47], suggests that one local quaternion frame among 3 frames is unphysical frame containing ghosts. In the case of phonon propagation, the conditions are different [29]. In (3+1)D, existence of hysteresis effects suggests presence of local quaternion times in the biquaternion framework.

In mathematics of lattice topology, there remain problems. A complex torus $T^2 = C^2/G$ where G is a discrete subgroup becomes a Hopf manifold $S^1 \times S^3$. Choosing $W = C^2 - (0, 0)$, $M = W/G = R/Z \times S^3$ is a Hopf manifold [10, 11], and one cannot impose Kähler structure, which is necessary for Hamiltonian dynamics. In projective space P^3 , one can identify $z \in W$ and $-z \in W$, one can impose Kähler structure. We start from TR symmetric space and consider appearance of a phase δ from non-commutativity of $q_1, q_2 \in S^3$ as $q_1 q_2 = q_2 q_1 e^{\sqrt{-1}\delta}$.

The loop depends on the time sequence (t_1, t_2, \dots, t_m) , but patching neighborhoods of the local coordinate $(z_j, t) = (z_j^1, z_j^2, t_1, \dots, t_m)$ defined as the patch U_j is shown to be independent of the time series t_1, \dots, t_m in P^3 .

The algebra $\mathcal{A}_{4,1}$ is isomorphic to $M_2(\mathbf{H}) \oplus M_2(\mathbf{H})$

$$j(\mathcal{A}_{4,1}) = \begin{pmatrix} x_2 \mathbf{i} + x_3 \mathbf{j} + x_4 \mathbf{k} & -x_1 + x_5 \\ x_1 + x_5 & -x_2 \mathbf{i} - x_3 \mathbf{j} - x_4 \mathbf{k} \end{pmatrix}$$

where x_i are real.

In the Light Front Quantum Chromo Dynamics(LFQCD) of Srivastava and Brodsky [32, 33] $\tau = (t - z/c)/\sqrt{2}$ corresponds to $(x_1 - x_5)/\sqrt{2}$. For massless particle, propagators are doubly transverse, i.e. with respect to the gauge direction n_μ and the chirality direction k_μ .

The two $M_2(\mathbf{H})$ represent TR symmetric physical fields, and the BRST ghost fields are decoupled.

In the FP lattice simulation, fermion propagation direction and its orthogonal 2D plane can be characterized by quaternions. If a generalization of Castro et al.'s Fourier transform[2] becomes possible, a progress of the quaternion quantum field theory would occur.

Bosonic wave propagations in Weyl fermion background and in Dirac fermion background are different. The former is suitable for detecting chiral U(1) symmetry and the latter is suitable for detecting charge U(1) symmetry.

The Clifford algebra bases for $\mathcal{A}_{3,1}$ were taken from Garling [24], but there are differences in definition of time. The time axis e_1e_4, e_2e_4 and e_3e_4 are contained symmetrically. Our model has qualitative differences between the combination of e_0 and e_3e_4 and e_0 and e_1e_4, e_2e_4 . The paths $L21 - L24$ contain different path e_ie_4 and $-e_ie_4$. We extended the Vahlen transformation on a (2+1)D Clifford algebra given by Porteous[22] to (3+1)D Clifford algebra, and changed the Möbius transformation matrix element xx^- to $\sum_{i=1}^3 X_i \bar{X}_i$.

There are three quaternion local times in contrast to one local quaternion time postulated by Ariel[8, 9]. When there are hysteresis effects, it might be necessary to consider Möbius band structure.

Acknowledgments

The author thanks Prof. S. Dos Santos for valuable discussions on SVD and transferring the article[12], and the Laboratory for Industrial Research (Nissanken) for the financial aid to the travel expense to INSA in November. The author is grateful to Prof. S.J. Brodsky, Prof. E. Hitzer and Prof. V. Ariel for helpful communication, Prof. M. Arai and Prof. K. Hamada for allowing the use of a workstation as their research collaborator, and Mr. Wu in the laboratory for helps in Python programmings. Thanks are also due to the library of the Tokyo Institute of Technology and that for mathematical science of the University of Tokyo for allowing consultation of references.

References

- [1] E. Hitzer, *Quadratic Phase Quaternion Domain Fourier Transform*, in Bin Sheng et al. (eds) Advances in Computer Graphics, CGI 2023. LNCS, vol14498, Springer (2023).
- [2] L.P. Castro, I.T. Minh and M.N. Tuan, *New Convolutions for Quadratic-Phase Fourier Integral Operators and their Applications*, Mediterr.J. Math **15** 13(2018).
- [3] E. Hitzer and S.J. Sangwine, *The orthogonal 2D Plane Split of Quaternions and Steerable Quaternion Fourier Transformations*, in E. Hitzer and S.J. Sangwine (Eds.) Quaternion and Clifford Fourier Transform and Wavelets, Trends in Mathematics (TIM) **27**, Birkhäuser, 2013, pp.15-40;arXiv: 1306.2157v1 (2013).
- [4] E. Hitzer, *Quaternion and Clifford Fourier Transforms*, CRC Press, Boca Raton, London, New York (2022).
- [5] S.L. Adler, *Quaternionic Quantum Field Theory*, Phys. Rev. Lett. **55** (8) 783-786 (1985). Errata **55** (13) 1430 (1985).
- [6] S.L. Adler, *Quaternionic Quantum Field Theory*, Commun. Math. Phys, **104**, 611-656 (1986)
- [7] É. Cartan, *The Theory of Spinors*, Dover Publishing (1966).
- [8] V. Ariel, *Quaternion Space-Time and Matter*, arXiv:2106.06394v1[physics.gen-ph]
- [9] V. Ariel, *Elements of Time*, Journal of Modern Physics, **14** 1537-1561 (2023).
- [10] K. Kodaira, *Theory of Complex Manifolds* (in Japanese) , Iwanami Pub. Tokyo (1992).
- [11] H. Hopf, *Über die Abbildungen von Sphären auf Sphären niedriger Dimension*, Fundamenta Mathematicae, Warsaw: Polish Acad. Sci., **25**:427-440 (1932).
- [12] S. Miran, J. Flamant, N. Le Bihan, P. Chainais, and D. Brie, *Quaternion in Signal and Image Processing A comprehensive and objective overview*, IEEE Signal Processing Magazine **40** (6) (2023).
- [13] M. Felsberg and G. Sommer, *The Monogenic Signal* IEEE. Trans. Signal Proc. **49** (12) (2001).

- [14] M. Unser, D. Sage and D. Van De Ville, *Multiresolution Monogenic Signal Analysis Using the Riesz-Laplace Wavelet Transform*, IEEE Trans. Image Proc. **18** (11) (2009).
- [15] Wikipedia, *Short-time Fourier Transform*, Wikipedia (2023).
- [16] S. Furui and S. Dos Santos, *Application of Quaternion Neural Network to Time Reversal Based Nonlinear Elastic Wave Spectroscopy*, INAE, **8** 183-199, (2023).
- [17] E. Hitzler, *The Quaternion Domain Fourier Transform and its Properties*, Adv. Appl. Clifford Algebras **26** 969-984 (2016).
- [18] F.J. Dyson, *Correlations between Eigenvalues of a Random Matrix*, Commun. Math. Phys. **19** 235-250 (1970).
- [19] P. Lounesto, *Clifford Algebras and Spinors*, Second Edition, Cambridge University Press, Cambridge (2001).
- [20] J. Vaz Jr, *The Clifford algebra of physical space and Dirac theory*, IOP Publishing, Eur. J. Phys. **37** 055407 (2016).
- [21] K. Th. Vahlen, *Ueber Bewegungen und complex Zahlen*, Math. Ann. **55** 585-593 (1902).
- [22] L.R. Porteous, *Clifford Algebras and the Classical Groups*, Cambridge University Press (1995).
- [23] D. Hestenes, *Quantum Mechanics of the electron particle-clock*, arXiv:1910.10478v2 [physics.gen-ph] (2020).
- [24] D.J.H. Garling, *Clifford Algebras: An Introduction*, Cambridge University Press (2011).
- [25] M. Lints, A. Saupere and S. Dos Santos, *Formation and Detection of Solitonic Waves in Dilatant Granular Materials: Potential Application for Nonlinear NDT*, NDT.net.Issue:2014-1182014).
- [26] S. Furui and S. Dos Santos, *Monte Carlo simulation of phonon propagation in the Fermi-sea of Weyl spinors and detection of hysteresis effects using Groupoids*, arXiv:1301.2095 v3 (2021).

- [27] S. Furui and S. DosSantos, *Clifford Fourier Transforms in (2+1)D Lattice Simulations of Soliton Propagations*, PoS Lattice22, The 39th International Symposium on Lattice Field Theory, 8th-13th August, 2022, Rheinische Friedrich-Wilhelms-Universität Bonn, Bonn, Germany, arXiv:[hep-lat physics.comp-ph]
- [28] S. Furui, *Solving Nonlinear Dynamics using Path-integral methods and Machine Learning techniques, - Paths of Phonetic Solitons in (2+1) D and Paths of Hadrons in (4+2) D space-time-*, in preparation.
- [29] S. Furui and S. Dos Santos, in preparation.
- [30] J. Papouskova, V. Kus and S. Dos Santos, *Preisach-Mayergoyz space model density identification for nonlinear physical systems: "L-2" and "D-divergence" minimization methods*, Proceedings of Meetings on Acoustics, **16**, 045018 (2012).
- [31] Z. Dvorakova, S. Dos Santos, V. Kus and Z. Prevolsky, *Localization and Classification of scattered nonlinear ultrasonic signatures in bio-mechanical media using time reversal approach*, J. Acoust. Soc. Am. **154** (3) pp.1684-1695 (2023).
- [32] P. Srivastava and S. J. Brodsky, *Light-front-quantized QCD in the light-cone gauge: The doubly transverse gauge propagator*, Phys. Rev. **D 64**, 045006 (2001).
- [33] P. Srivastava and S. J. Brodsky, *Light-front formulation of the standard model*, Phys. Rev. **D 66**, 045019 (2002).
- [34] T. DeGrand, A. Hasenfratz, P. Hasenfratz and F. Niedermayer, *Non-perturbative tests of the fixed point action for SU(3) gauge theory*, Nucl. Phys.**B454** 615-637 (1995), arXiv:9506031[hep-lat].
- [35] S. Ito, *Introduction to Lebesgue Integrals* (in Japanese), Shokabou Pub. Tokyo (1965).
- [36] M. Levin and C.P. Nave, *Tensor Renormalization Group Approach to Two-Dimensional Classical Lattice Models*, Phys. Rev. Lett. **99**, 120601 (2007).
- [37] Z.Y. Xie, J. Chen, M.P. Qin, J.W. Zhu, L.P. Yang and T. Xiang, *Coarse-graining renormalization by higher-order singular value decomposition*, Phys. Rev. **B 86**,045139 (2012).

- [38] D. Adachi, T. Okubo and S. Todo, *Anisotropic tensor renormalization group*, Phys. Rev. **B** **102**, 054432 (2020).
- [39] S. Akiyama, *Bond-weighting methods for the Grassmann tensor renormalization group*, arXiv:2208.03227v2 (2022).
- [40] A. Yosprakob, *GrassmannTH: a Python package for Grassmann tensor network computations*, arXiv:2309.07557v1(2023).
- [41] A. Yosprakob, J. Nishimura and K. Okunishi, *A new technique to incorporate multiple fermion flavors in tensor renormalization group method for lattice gauge theories*, arXiv:2309.01422 v2[hep-lat].
- [42] A. Gray, E. Abbena and S. Salamon, *Modern Differential Geometry of curves and Surfaces with Mathematica*, Chapman and Hall/CRC (2006).
- [43] M.P. Atiyah, R. Bott and A. Shapiro, *Clifford Modules*, Topology **3**, Suppl. 1,3-38 (1963).
- [44] A.N. Kolmogorov and S.V. Fomin, *Introductory Real Analysis*, (translated to Japanese by M. Yamazaki) Iwanami Pub. Tokyo (1965).
- [45] J. Horváth, *Topological Vector Spaces and Distributions* vol. I, Addison-Wesley, Reading, Massachusetts (1966).
- [46] Japan Mathematical Society, *Dictionary of Mathematics* 2nd edition, (in Japanese), Iwanami Pub. Tokyo (1970).
- [47] R. Avila, J.R. Nascimento, A.Y. Petrov, C.M. Reyes and M. Schreck, *Causality, unitarity and indefinite metric in Maxwell-Chern-Simons extensions*, Phys. Rev. **D101**,055011 (2020).